

Weak population structure and recent demographic expansion of the monogenean parasite *Kapentagyrus* spp. infecting clupeid fishes of Lake Tanganyika, East Africa

Peer-reviewed author version

KMENTOVA, Nikol; Koblmuller, S; VAN STEENBERGE, Maarten; Raeymaekers, JAM; ARTOIS, Tom; De Keyzer, ELR; MILEC, Leona; Bukinga, FM; N'sibula, TM; Mulungula, PM; Ntakimazi, G; Volckaert, FAM; Gelnar, M & VANHOVE, Maarten (2020) Weak population structure and recent demographic expansion of the monogenean parasite *Kapentagyrus* spp. infecting clupeid fishes of Lake Tanganyika, East Africa. In: *International Journal for Parasitology*, 50 (6-7) , p. 471 -486.

DOI: 10.1016/j.ijpara.2020.02.002

Handle: <http://hdl.handle.net/1942/31463>

1 **Weak population structure and expansive demographic history of the monogenean**  
2 **parasite *Kapentagyris* spp. infecting clupeid fishes of Lake Tanganyika**

3 **Nikol Kmentová<sup>1,2,3\*</sup>, Stephan Koblmüller<sup>4</sup>, Maarten Van Steenberge<sup>3,4,5,6</sup>, Joost A.M.**  
4 **Raeymaekers<sup>7</sup>, Tom Artois<sup>2</sup>, Els L.R. De Keyzer<sup>3,8</sup>, Leona Milec<sup>7</sup>, Fidel Muterezi Bukinga<sup>9</sup>, Théophile**  
5 **Mulimbwa N'sibula<sup>9</sup>, Pascal Masilya Mulungula<sup>9</sup>, Gaspard Ntakimazi<sup>10</sup>, Filip A.M. Volckaert<sup>3</sup>,**  
6 **Milan Gelnar<sup>1</sup>, Maarten P.M. Vanhove<sup>1,2,3,11</sup>**

7 <sup>1</sup> Department of Botany and Zoology, Faculty of Science, Masaryk University, Kotlářská 2, 611 37  
8 Brno, Czech Republic

9 <sup>2</sup> Hasselt University, Centre for Environmental Sciences, Research Group Zoology: Biodiversity &  
10 Toxicology, Agoralaan Gebouw D, B-3590 Diepenbeek, Belgium

11 <sup>3</sup> Laboratory of Biodiversity and Evolutionary Genomics, Department of Biology, University of  
12 Leuven, Ch. Deberiotstraat 32, B-3000 Leuven, Belgium

13 <sup>4</sup> Institute of Biology, University of Graz, Universitätsplatz 2, A-8010 Graz, Austria

14 <sup>5</sup> Operational Directorate Taxonomy and Phylogeny, Royal Belgian Institute of Natural Sciences,  
15 Vautierstraat 29, B-1000 Brussels, Belgium

16 <sup>6</sup> Biology Department, Royal Museum for Central Africa, Leuvensesteenweg 13, 3080, Tervuren,  
17 Belgium

18 <sup>7</sup> Faculty of Biosciences and Aquaculture, Nord University, N-8049 Bodø, Norway

19 <sup>8</sup> Capacities for Biodiversity and Sustainable Development (CEBioS), Operational Directorate Natural  
20 Environment, Royal Belgian Institute of Natural Sciences, Vautierstraat 29, B-1000, Brussels,  
21 Belgium

22 <sup>9</sup> Centre de Recherche en Hydrobiologie, Département de Biologie, B.P. 73 Uvira, Democratic  
23 Republic of Congo

24 <sup>10</sup> Département de Biologie, Université du Burundi, Campus Mutanga, B.P. 2700, Bujumbura,  
25 Burundi

26 <sup>11</sup> Zoology Unit, Finnish Museum of Natural History, University of Helsinki, P.O.Box 17, Helsinki FI-  
27 00014, Finland

28 \*corresponding author: kmentovan@mail.muni.cz, Laboratory of Parasitology, Department of  
29 Botany and Zoology, Masaryk University, Kamenice 5, 625 00 Brno, Czech Republic

30 Note: Supplementary data associated with this article

31

32

33

34

35

36

37

38

39

40

41

42

43

44

45

46 **Abstract**

47 Lake Tanganyika is the oldest and deepest African Great Lake and harbours one of the most  
48 diverse fish assemblages on earth. Two clupeid fishes, *Limnothrissa miodon* and *Stolothrissa*  
49 *tanganicae*, constitute a major part of the total fish catch, making them indispensable for local  
50 food security. Parasites have been proposed as indicators of stock structure in highly mobile  
51 pelagic hosts. We examined the monogeneans *Kapentagyris limnothrissae* and *K. tanganicanus*  
52 (Dactylogyridae) infecting these clupeids to explore the parasites' lake-wide population structure  
53 and patterns of demographic history.

54 Samples were collected at seven sites distributed across three subbasins of the lake. Intraspecific  
55 morphological variation of the monogeneans (N = 380) was analysed using morphometrics and  
56 geomorphometrics of sclerotised structures. Genetic population structure of both parasite species  
57 (N = 246) was assessed based on a 415 bp fragment of the mitochondrial COI gene.

58 Overall, we observed a lack of clear geographical morphological differentiation in both parasites  
59 along a north-south axis. This lack of geographical population structure was also reflected by a  
60 large proportion of shared haplotypes, and a pattern of seemingly unrestricted gene flow between  
61 populations. Significant morphological and genetic differentiation between some populations  
62 might reflect temporal differentiation rather than pure geographical isolation. Overall, the shallow  
63 population structure of both species of *Kapentagyris* reflects the near-panmictic population  
64 structure of both host species reported in previous studies. Morphological differences related to  
65 host species identity of *K. tanganicanus* were consistent with incipient speciation observed at the  
66 genetic level. Both parasite species experienced a recent demographic expansion, which might be  
67 linked to paleohydrological events. Finally, hybridisation between species of *Kapentagyris* was  
68 found, representing the first case in dactylogyrid monogeneans.

69 **Keywords:** Clupeidae, Dactylogyridae, Fisheries target species, *Kapentagyrus limnotrissae*,  
70 *Kapentagyrus tanganicanus*, Phenotypic plasticity, Population genetics  
71

## 72 **1. Introduction**

73 The pelagic realm of the African Great Lakes harbours a lower species diversity than the littoral  
74 habitat. This might be attributed to the lower number of niches and a lack of barriers to gene flow  
75 (Kirchberger et al., 2012; Shaw et al., 2000). Lake Tanganyika's pelagic zone is dominated by two  
76 clupeid species (*Limnothrissa miodon* (Boulenger, 1906) and *Stolothrissa tanganicae* Regan, 1917)  
77 and their latid fish predators. The two clupeids make up 65% (in mass) of the total catch in Lake  
78 Tanganyika, making them a key component of the local fishery and an important factor for the  
79 food security in the countries bordering the lake (Mölsä et al., 1999). Clupeids play an important  
80 role in the food chain, because they are a link between the plankton and the piscivores (Coulter,  
81 1991). Lake Tanganyika clupeids are parasitized by two species of *Kapentagyris* Kmentová, Gelnar  
82 & Vanhove, 2018 (Monogenea, Dactylogyridae), *Kapentagyris limnothrissae* (Paperna, 1973) and  
83 *Kapentagyris tanganicanus* Kmentová, Gelnar & Vanhove, 2018. Both parasite species have a  
84 lake-wide distribution throughout the year (Kmentová et al., 2018). While *K. limnothrissae* is host  
85 specific to *L. miodon*, *K. tanganicanus* has a more generalist lifestyle and infects both *L. miodon*  
86 and *S. tanganicae*. In *K. tanganicanus*, two distinct morphotypes related to sardine species identity  
87 have been observed (Kmentová et al., 2018).

88 Clupeids in Lake Tanganyika are short-lived species with a lifespan of usually one year and  
89 maximally three years. Other biological characteristics include schooling behaviour and a diurnal  
90 vertical migration that follows that of zooplankton (Coulter, 1991; Mulimbwa and Shirakihara,  
91 1994). Migration and population connectivity of clupeids in the lake are poorly understood, but  
92 are thought to be linked to seasonal changes in the plankton distribution (Kurki et al., 1999;  
93 Plisnier et al., 2009). Generally, the delineation of pelagic fish stocks is crucial for fisheries  
94 management (Emmett et al., 2005). Classical methods to track the movement of fish populations,  
95 such as data storage tags (DST) and passive physical tags are no option for clupeids because of

96 their fragility (James et al., 1988). Hence, a combination of biological markers such as  
97 morphometry, parasites, otolith elemental profiles, and molecular markers appears to be a more  
98 promising approach (Svedäng et al., 2010). Lake-wide genome screening of both clupeids in Lake  
99 Tanganyika using SNPs did not identify a clear population structure, suggesting near-panmictic  
100 populations (De Keyzer et al., 2019; Junker et al., 2019). However, differences in chemical  
101 composition of otoliths in both species (Sako et al., 2005) and a pattern of isolation by distance  
102 along a north-south gradient in *S. tanganyicae* (De Keyzer et al., 2019) pointed to restricted long-  
103 distance migration.

104 A combination of host- and parasite genetics has been proposed as an integrative approach to  
105 reconstruct host population structure (Catalano et al., 2014) or stock structure over small  
106 geographical and temporal scales (Baldwin et al., 2012). Monogenean parasites are excellent  
107 targets for such research for several reasons. Foremost, the direct life cycle and often high host  
108 specificity of monogeneans prevents their life history from being influenced by any other than the  
109 targeted host taxon (Catalano et al., 2014; Pariselle et al., 2011). Secondly, due to their short  
110 generation time, monogeneans may accumulate genetic changes more rapidly than their hosts  
111 (Poulin, 2007). Thirdly, their high mutation rate in comparison to that of their hosts may reflect  
112 historical events that are too recent to be inferred from host genetics (Nieberding et al., 2004;  
113 Nieberding and Olivieri, 2007), and therefore parasites have been proposed to act as a  
114 “magnifying glass” for their hosts. To date, few studies have used monogeneans in such an  
115 approach. E.g., Pettersen et al. (2015) used a portion of the cytochrome c oxidase of *Gyrodactylus*  
116 *thymalli* Žitňan, 1960 combined with dehydrogenase subunit 5 to indirectly infer barriers to gene  
117 flow in grayling (*Thymallus thymallus* L.). Monogenean genetics was also used to track the  
118 historical distribution of clariid catfishes in Africa (Barson et al., 2010) as well as to reconstruct  
119 introduction pathways in *Perccottus glenii* Dybowski, 1877 (Ondračková et al., 2012).

120 Several steps have to be considered before using parasites as tags for host population structure,  
121 including parasite species identification, the availability of more than one genetic marker to verify  
122 cryptic species, and temporal stability in the presence of the parasite species across the host's  
123 geographic range (Mattiucci et al., 2004; Vilas et al., 2005). All above-mentioned criteria are  
124 fulfilled in the system studied here. Since the morphology of their sclerotised structures was  
125 shown to vary along a north-south gradient (Kmentová et al., 2018), the species of *Kapentagyrus*  
126 are proposed as candidates for unravelling the clupeids' population structure in Lake Tanganyika.  
127 Moreover, several periods of draught in the past led to low lake levels and at times even  
128 separation into up to four paleolakes corresponding with the current subbasins (Danley et al.,  
129 2012; Sturmbauer et al., 2017). Such events repeatedly caused periods of population separation  
130 followed by periods of secondary admixture across the north-south gradient. These left their  
131 signature in the genetics of various animal taxa (Sturmbauer et al., 2001) and influenced their  
132 current population structure (Nevado et al., 2013; Sefc et al., 2017; Sturmbauer et al., 2017), or  
133 their demographic history, even in the barrier-free pelagic realm (Koblmüller et al., 2019). We  
134 assume that the demographic history of *Kapentagyrus* spp. is connected with past population  
135 trajectories of clupeid hosts, because historical lake level fluctuations influenced the demographic  
136 history of cichlid fishes and their respective monogenean species in a similar way (Kmentová et al.,  
137 2016; Koblmüller et al., 2019).

138 In this study, we test two species of *Kapentagyrus* as potential markers for spatio-temporal  
139 population structure of both clupeid species. We hypothesise that there is more differentiation  
140 among parasite populations than among host populations. We also compare the degree of  
141 morphological and genetic differentiation among a host-specific versus a more generalist species  
142 of *Kapentagyrus*. Finally, we test the relation between the hydrological history of Lake Tanganyika  
143 and the recent demographic history of *Kapentagyrus* spp.



144 **2. Material and methods**

145 2.1. Sampling design

146 In total, 380 monogenean individuals collected from 497 host specimens were morphologically  
147 analysed in this study. We used samples listed in Kmentová et al. (2018) as well as new specimens  
148 collected in April 2018 (see Table 1). Monogeneans were collected from ethanol-preserved fish  
149 samples collected along the lake's shoreline within two days in April 2018 (off Bujumbura,  
150 Kalemie, Mpulungu and Uvira). As clupeids are highly mobile pelagic fish (De Keyzer et al., 2019;  
151 Marshall, 1993; Mulimbwa and Mannini, 1993), this short time window enabled us to analyse the  
152 spatial population structure of the parasites without the potential effect of school migration.  
153 Additionally, fresh specimens collected within two days in August 2016 (off Kalemie and Uvira) and  
154 within two weeks in Mpulungu 2018 were included in this study to analyse spatio-temporal  
155 patterns in the parasites' morphology. We also included fresh specimens collected at Baraka in  
156 2017, Mpulungu in 2016, Mvugo in 2016 and Mvuna Island in 2015 to increase spatial resolution  
157 of population genetic analyses. In total, 246 individuals of *Kapentagyris* spp. were characterised  
158 genetically (see Table 1).

159 All host specimens were either bought at fish markets in the above-mentioned cities or caught  
160 with gills nets during experimental fishing. Fishes were identified to species level *in situ*. Voucher  
161 specimens of the two clupeid species are part of the ichthyology collection of the Royal Museum  
162 for Central Africa in Tervuren (RMCA 2016.20). Monogenean individuals collected from fresh fish  
163 specimens were placed on a slide in a drop of glycerine ammonium picrate solution (GAP) in 1:1  
164 ratio. Ethanol-preserved samples were cleaned of host tissue in a drop of water followed by  
165 adding Hoyer's solution. In both cases, the individuals were fixed under a cover slip. All collected  
166 monogenean species were identified as either *K. limnotrissae* or *K. tanganicus*. Infection  
167 parameters are listed in Table 1. Voucher specimens of *Kapentagyris* spp. are deposited in the

168 collection of the Research Group Zoology: Biodiversity and Toxicology at Hasselt University in  
169 Diepenbeek, Belgium (HU) (see Table 1 for accession numbers).

## 170 2.2. Morphometrics and geomorphometrics

171 Morphological variation on a lake wide geographical scale was inferred via both morphometric  
172 and geomorphometric approaches. Haptoral and male copulatory hardparts of the two species of  
173 *Kapentagyris* were measured and photographed using an Olympus BX51 microscope with  
174 incorporated phase contrast at a magnification of 1000x (objective x100 immersion, ocular x10)  
175 with *MicrolImage* v3.1. In total, we obtained 23 different morphometric parameters following the  
176 terminology of Řehulková et al. (2013).

177 Geomorphometric data were obtained by digitising the shape of the dorsal and ventral anchor,  
178 respectively. For this we used *tps Dig* v2.30 from the thin-plate spline (TPS) packages (Rohlf, 2006).  
179 We chose the anchors for geomorphometric analyses as their shape had been successfully used in  
180 intraspecific studies on members of *Ligophorus* Euzet & Suriano, 1977 (Monogenea,  
181 Dactylogyridae) (Rodríguez-González et al., 2015). The shape of other monogeneans' sclerotised  
182 structures, such as the shape of bars and marginal hooks, was shown to be highly related to the  
183 method of sample preparation (Vignon et al., 2011). Eight fixed landmarks were selected on each  
184 of the anchors. Additionally, semi-landmarks were placed in equal intervals on each anchor,  
185 resulting in 98 of them in the case of *K. limnotrissae* and 102 in *K. tanganicanus* (see Fig S1).

## 186 2.3. DNA extraction and genetic characterisation

187 Monogeneans were stored in 99% ethanol prior to DNA isolation. Subsequently, ethanol was  
188 evaporated using a vacuum centrifuge and lysis buffer was poured onto the specimens. Whole  
189 genomic DNA was extracted using either the Qiagen DNeasy Blood & Tissue Kit or Nucleospin

190 Tissue Genomic DNA kit following the manufacturer's instructions. The extracted DNA was eluted  
191 in a volume of 50 µl.

192 Part of the monogenean mitochondrial cytochrome c oxidase subunit 1 (COI) gene was amplified  
193 using a nested PCR reaction, in view of the low content of genomic DNA extracted from in most  
194 cases 1/3 of the worm. The first PCR reaction was performed with ASmit1 (5'-  
195 TTTTTTGGGCATCCTGAGGTTTAT-3') (Littlewood et al., 1997) and Schisto3 (5'-  
196 TAATGCATMGGAAAAAACA-3') (Lockyer et al., 2003) primers in 24 µl of PCR mix (one unit of *Taq*  
197 Polymerase, 1X buffer containing 2 mM MgCl<sub>2</sub>, 0.2 mM dNTPs, 0.8 mM of each primer) for a total  
198 reaction volume of 25 µl. It was carried out under the following conditions: initial denaturation at  
199 95°C for 5 min, then 40 cycles of 1 min at 94°C, 1 min at 50°C and 1 min at 72°C, and final  
200 elongation for 7 min at 72°C. The nested PCR with ASmit1 and ASmit2 (5'-  
201 TAAAGAAAGAACATAATGAAAATG-3') (Littlewood et al., 1997) primers followed the same protocol  
202 as the first one with 1:100 dilution of template DNA. The final PCR products were enzymatically  
203 purified using 1 µl of ExoSAP-IT reagent and 2.5 µl of PCR product under the following conditions:  
204 15 min at 37 °C and 15 min at 80 °C. The same primers as in the amplification reactions were used  
205 for sequencing with a BigDye Terminator® Cycle Sequencing Kit v3.1 (ThermoFisher Scientific),  
206 following the manufacturer's recommendations. The fragments were cleaned up using the BigDye  
207 XTerminator® Purification Kit (ThermoFisher Scientific) and visualized on an ABI 3130 capillary  
208 sequencer (Applied Biosystems).

209 For *S. tanganycae*, sequences of the mitochondrial cytochrome c oxidase subunit I (COI) gene were  
210 obtained from De Keyzer et al. (2019) (GenBank accession numbers MH290064-159). For *L.*  
211 *miodon*, DNA was extracted from finclips using the NucleoSpin Tissue kit (Macherey-Nagel GmbH)  
212 according to the manufacturer's instructions. Subsequently, the COI gene was amplified using the  
213 universal primer combination HCO2198 (5'-TAAACTTCAGGGTGACCAAAAATCA-3') and LCO1490  
214 (5'-GGTCAACAAATCATAAAGATATTGG-3') (Folmer et al., 1994). PCR reaction was performed in 24

215  $\mu$ l of PCR mix (12.5 $\mu$ l MyTaq HS mix (2x) (Bioline, London, UK), 10.5 $\mu$ l H<sub>2</sub>O and 1 $\mu$ l primer mix  
216 (20 $\mu$ M of each primer) to which 1  $\mu$ l of purified DNA was added for a total reaction volume of 25  
217  $\mu$ l (Handy et al., 2011). It was carried out under the following conditions: initial denaturation at  
218 94°C for 3 min, then 35 cycles of 45 sec at 94°C, 40 sec min at 52°C and 90 sec at 72°C, and final  
219 elongation for 10 min at 72°C. PCR products were purified using CleanPCR beads (CleanNA, GC  
220 Biotech). The same primers as in the amplification reactions were used for sequencing with a  
221 BigDye Terminator® Cycle Sequencing Kit v3.1 (ThermoFisher Scientific), following the  
222 manufacturer's recommendations. The fragments were purified CleanDTR beads (CleanNA, GC  
223 Biotech) and visualized on an ABI 3500XL capillary sequencer (Applied Biosystems).  
224 DNA sequences were visually inspected and corrected using MEGA v7 (Kumar et al., 2016) and  
225 aligned using MUSCLE (Edgar, 2004) under default distance measures as implemented in MEGA.  
226 COI sequences of *Kapentagyris* spp. are deposited in NCBI GenBank under the accession numbers  
227 MK598125-323. Corresponding nuclear data generated by Kmentová et al. (2018) are available on  
228 NCBI GenBank under the accession numbers MH071782 and MH071808 (28S, 18S and ITS-1 region  
229 of *K. limnotrissae*), MH071783 and MH071807 (28S, 18S and ITS-1 region of *K. tanganicanus*  
230 collected from *L. miodon*), MK522517-520 (28S, 18S and ITS-1 region of *K. tanganicanus* collected  
231 from *Stolothrissa tanganicæ*), MK521656-MK521659 (28S rDNA portion of *K. limnotrissae*  
232 individuals identified as hybrids) and MK521661-MK521664 (18S and ITS-1 rDNA portion of *K.*  
233 *limnotrissae* individuals identified as hybrids). COI sequences of *L. miodon* are deposited in NCBI  
234 GenBank under the accession numbers MT040511-78. Individuals of both host species originate  
235 from different localities covering all three major subbasins of Lake Tanganyika (see Table S1).

236

## 237 2.4. Data analysis

238

### 239 2.4.1. Morphological differentiation

240 To avoid any possible influence of ethanol fixation on the size and shape of sclerotised structures,  
241 the samples were subdivided into spatial (ethanol-preserved) and spatio-temporal (fresh) data  
242 sets. To evaluate intraspecific and intrahost variation, data sets were further subdivided into six  
243 different sample sets according to parasite species and host species. These sample sets were  
244 always analysed separately by a) morphometric analyses of haptoral structures, and  
245 geomorphometric analyses of b) dorsal and c) ventral anchors. Samples in all sample sets and  
246 subsequent analyses were grouped by sampling site to check for possible geographical structure in  
247 both species of *Kapentagyris*. As preliminary analyses indicated a significant influence of host size  
248 on morphological characters, individuals of *K. tanganicus* ex *L. miodon* from Kalemie 2018 were  
249 analysed as two groups using 12 cm of host standard length (SL) as a cut off value (referred to as  
250 Kalemie 2018 Big and Kalemie 2018 Small, respectively). As the same pattern was discovered with  
251 the fresh samples from Mpulungu, a threshold in SL of host specimens was set to 10 cm (referred  
252 to as Mpulungu 2018 Big and Mpulungu 2018 Small, respectively).

253 *Morphometrics* - Principal component analysis (PCA) of haptoral morphometric parameters  
254 standardised to unit scale was performed in the R package *ade4* (Jombart, 2008). Missing data  
255 were replaced by the average value for each morphological character. To increase the resolution  
256 of the resulting pattern, morphological characters with more than 50% missing data were  
257 excluded prior to the analysis. Then, linear or generalised linear models were calculated in the R  
258 package *stats* (R Core Team, 2013) to evaluate the effect of sampling site, host size and their  
259 interaction on each of the morphological characters followed by F-statistic and Chi Square  
260 statistics, respectively. In case of an overall significant effect of sampling site, *post hoc* Welch's t  
261 test and Tukey test, respectively, were performed to assess pairwise significance between  
262 sampling sites. Sampling sites with insufficient number of specimens (< 10) were excluded from  
263 the analyses.

264 *Geomorphometrics* - Configurations of fixed landmarks were superimposed using Generalized Full  
265 Procrustes Analyses (Cox and Cox, 1989; Zelditch et al., 2012), under the Least Squares criterion to  
266 minimize bending energy with respect to a mean reference shape. Canonical variate analyses  
267 (CVA) (Klingenberg and Monteiro, 2005) and PCA using only the fixed landmarks were performed  
268 in *MorphoJ* v2.0 (Klingenberg, 2011). A permutation test with 10,000 iterations was used to  
269 statistically validate pairwise differences between the pre-defined groups. Additionally, the overall  
270 shape of both anchors, captured using fixed landmarks and semi-landmarks, was analysed using  
271 *tpsRelw* v1.49. A Relative Warp Analysis (RWA) (Rohlf, 1993) was performed with the Procrustes  
272 coordinates. The scaling option was set to  $\alpha = 0$  to give all landmarks equal weight. Sampling sites  
273 with insufficient number of specimens (<6 as in the case of *K. tanganicanus* ex *L. miodon* from  
274 Bujumbura 2018 and *K. tanganicanus* ex *S. tanganiccae* from Bujumbura 2018 and Mpulungu 2018  
275 in spatial sample sets) were excluded from the analyses.

276 Relationships between the individual scores inferred with PCA and RWA analyses, respectively,  
277 and the host size were checked via linear regression analyses in the R package *stats* (R Core Team,  
278 2013). This was done for each sample set and within the respective groups. All sample sets were  
279 visually inspected for outliers, which were excluded from the analyses. Normality of the data was  
280 checked by Shapiro-Wilks tests in the R package *onewaytests* (Dag et al., 2018). The homogeneity  
281 of variance among groups within each sample set was assessed by Levene's tests in the R package  
282 *car* (Fox and Weisberg, 2011). Biplots of PC and RW scores were visualised with the packages  
283 *ggplot2* (Wickham, 2009) and *factoextra* (Kassambara and Mundt, 2017).

#### 284 2.4.2. Genetic structure

285 The genetic diversity of the two monogenean species and the two host species was studied based  
286 on 415 bp (*Kapentagyryus* spp.), 646 bp (*L. miodon*) and 643 bp (*S. tanganiccae*), respectively, of the  
287 COI gene. Genetic diversity was assessed as the number of haplotypes and polymorphic sites,

288 haplotype diversity and nucleotide diversity, all calculated using *Arlequin* v3.5 (Excoffier and  
289 Lischer, 2010).

290 The genealogy of the COI haplotypes for the parasites were inferred by means of a Median Joining  
291 network in *PopART* v1.71 (Leigh and Bryant, 2015). Differentiation among pre-defined populations  
292 was estimated by  $F_{ST}$  in *Arlequin* v3.5 (Excoffier and Lischer, 2010): for *K. tanganicanus* collected  
293 from *L. miodon* and *S. tanganicæ*, respectively, in Uvira 2016, as well as for populations of *K.*  
294 *tanganicanus* ex *L. miodon* with at least 17 individuals available. Analysis of molecular variance  
295 (AMOVA) based on F-statistics was used to test for significant population structure of *K.*  
296 *tanganicanus* at the level of subbasins within Lake Tanganyika. Sample size for *K. limnotrissae* was  
297 generally too low to allow for any meaningful population genetic analyses.

#### 298 2.4.3. Demographic history

299 To test for signals of past population expansion in both species of monogeneans and their host  
300 species, two different neutrality test statistics, Tajima's D (Tajima, 1989) and Fu's  $F_s$  (Fu, 1997),  
301 were calculated in *Arlequin* v3.5 (Excoffier and Lischer, 2010).

302 The demographic history of *Kapentagyryus* spp. was further assessed by mismatch distribution  
303 analyses in *Arlequin* v3.5 (Excoffier and Lischer, 2010). The sum of square deviations (SSD) and  
304 raggedness index (rg) were used to assess the fit of the observed mismatch distributions to the  
305 expectations based on estimates of the growth parameter. Past population size trajectories of  
306 monogenean species were further investigated with a Bayesian skyline plot (Drummond et al.,  
307 2005), as implemented in *BEAST* v1.8.2. (Suchard et al., 2018). The substitution rate was set to  
308 10% per million years, which is lower than the rates previously used for viviparous gyrodactylid  
309 monogenean species characterised by asexual multiplication (Meinilä et al., 2004), and should  
310 take into account the assumed comparatively longer generation time and lower reproductive  
311 capacity of *Kapentagyryus* as oviparous dactylogyrid monogeneans (Tinsley, 2004). Two

312 independent MCMC runs of 300 million generations each and a sampling frequency of 30,000  
313 were conducted, with a burn-in of the first 10% of sampled generations. The number of grouped  
314 intervals was set to 5. Verification of effective sample sizes (ESS > 200 for all parameters), tracing  
315 MCMC runs and visualisation of past population size changes were done in *Tracer* v1.7 (Rambaut  
316 et al., 2018).

### 317 **3. Results**

#### 318 3.1. Morphological variation

##### 319 3.1.1. *Kapentagyryus limnotrissae* ex *Limnothrissa miodon*

320 Overall, the intraspecific morphological variation of *K. limnotrissae* was primarily affected by  
321 several parameters of the dorsal anchor, ventral anchor and branch length of the ventral bar (Fig.  
322 1B, Table S2). An overview of measurements from haptoral as well as from the male copulatory  
323 organ region is listed in Table S4.

324 *Haptoral structures* - PCA did not reveal any clear geographical separation based on haptoral  
325 morphometric parameters in *K. limnotrissae* along any of the PC axes in any of the two sample sets  
326 (Fig. 2A&B). However, differentiation was visible between the specimens from Mpulungu 2018  
327 and Uvira 2016 along the first and the second axis (Fig. 2B). In half of the comparisons between  
328 sampling sites tested, at least one of the morphological parameters was found to differ  
329 significantly. The length of the outer root of the ventral anchor was the only morphological  
330 character that differed between sampling sites in both sample sets (see Fig. 1 and Table S2).

331 *Dorsal and ventral anchor* - In *K. limnotrissae*, the PCA biplot based on fixed landmarks revealed a  
332 clearer differentiation between Uvira and Bujumbura 2018 for the dorsal than for the ventral  
333 anchor (Fig. 2C and Fig. S2A). This differentiation was further reflected in the CVA results (Table  
334 S3). The shape of the ventral anchor was significantly different between the specimens from Uvira



335 and Kalemie 2016, and between Kalemie 2016 and Mpulungu 2018 (detailed results presented in  
336 Table S2). The results of RWA (including sliding landmarks) confirmed the pattern obtained via PCA  
337 (Fig. S2).

338 *Effect of host size* - No effect of host size on the position of specimens in neither of the presented  
339 biplots was detected (not shown). Linear models for the spatial sample set revealed that the total  
340 length of the dorsal anchor decreased with host size ( $F_{1,58} = 5.32$ ,  $P < 0.05$ ). This was also the case  
341 for the point length of the dorsal anchor ( $\chi^2_{2,57} = 9.98$ ,  $P = 0.002$ ) in the spatio-temporal sample set.  
342 Linear models revealed an increasing effect of host size on the branch length of the dorsal bar  
343 ( $F_{2,60} = 9.17$ ,  $P < 0.05$ ) and the inner root length of the ventral anchor ( $\chi^2_{2,61} = 5.34$ ,  $P = 0.02$ ) in the  
344 spatio-temporal sample set.

#### 345 3.1.2. *Kapentagyris tanganicanus* ex *Limnothrissa miodon*

346 Overall, the intraspecific morphological variation in *K. tanganicanus* ex *L. miodon* was affected by  
347 several parameters of both the dorsal and the ventral anchor, the dorsal and the ventral bar as  
348 well as some of the pairs of marginal hooks (Fig. 1C, Table S2). An overview of measurements from  
349 the haptoral as well as the male copulatory organ region are given in Table S5.

350 *Haptoral structures* - The first PC axis of haptoral morphometric parameters revealed that  
351 specimens from Mpulungu 2018 were intermediate between those from Kalemie 2018 and Uvira  
352 2018 (Fig 3A). The separation was further reflected in the number of significantly different  
353 characters between the sampling sites (see Table S2). A separation was also visible along the first  
354 PC axis of haptoral morphometric parameters between specimens collected in Mpulungu 2018  
355 from those from Kalemie 2016 and Uvira 2016 (Fig. 3B). Only two morphological parameters  
356 differed significantly between Mpulungu 2018 and Uvira 2016 (see Table S2). A single one differed  
357 significantly between the two host-size categories from Kalemie 2018 and Mpulungu 2018.

358 *Dorsal and ventral anchor* - In *K. tanganicanus* ex *L. miodon*, the PCAs of the shape of both  
359 anchors, based on a fixed landmark geomorphometric approach, reflected the gradient visible in  
360 the biplot of the haptoral morphometric approach in the both spatial and the spatio-temporal  
361 sample sets (Fig. 3C-F). This differentiation was further supported by the CVA results. Here, a  
362 significant difference was observed in at least one of the anchors in comparisons between each of  
363 the sampling sites. The only exception was the comparison between Mpulungu 2018 and Uvira  
364 2018, where no difference was found (see also Table S3). Moreover, the shape of the ventral  
365 anchor and of both anchors differed significantly between the two host-size categories from  
366 Kalemie 2018 and Mpulungu 2018, respectively. The results of RWA (including sliding landmarks)  
367 confirmed the pattern obtained via PCA (Fig. S3).

368 *Effect of host size* - A significant effect of host size was detected only on the individual RW scores  
369 of the first axis for the ventral anchor of the spatio-temporal sample set ( $F_{1,64} = 7.08$ ,  $P = 0.010$ ).  
370 Linear models revealed an increasing effect of host size on the total length of the ventral anchor  
371 ( $F_{3,77} = 34.31$ ,  $P < 0.0010$ ) and the length to notch of the ventral anchor ( $\chi^2_{3,77} = 10.81$ ,  $P = 0.001$ ) in  
372 the case of spatio-temporal sample set.

### 373 3.1.3 *Kapentagyris tanganicanus* ex *Stolothrissa tanganicae*

374 Overall, the intraspecific morphological variation of *K. tanganicanus* ex *S. tanganicae* was affected  
375 by the length to notch of the dorsal anchor and the second pair of marginal hooks (Fig. 1D, Table  
376 S2). An overview of measurements from the haptoral as well as from the male copulatory organ  
377 region is listed in Table S6.

378 *Haptoral structures* - In total, two sample sets, both containing specimens of *K. tanganicanus* ex *S.*  
379 *tanganicae* from four and two different groups, respectively, were analysed. Clear differentiation  
380 was visible in the second PC axis of haptoral morphometric parameters between the specimens  
381 from Kalemie 2018 and Uvira 2018 (Fig. 4A). A single morphological character, the size of the first

382 pair of marginal hooks, differed significantly between sampling sites. Additionally, a separation in  
383 the spatio-temporal sample set was found between specimens from Mpulungu 2018 and Uvira  
384 2016 along the first and second PC axes (Fig. 4B). Similar to the previous sample set, only one  
385 morphological character, the length to the notch of the dorsal anchor, differed between sampling  
386 sites.

387 *Dorsal and ventral anchor* - The position of specimens along the first PC axis of the anchor shape  
388 based on a fixed landmark geomorphometric approach mirrored the pattern observed in haptoral  
389 morphometric characters in both sample sets (Fig. 4C-F). In the spatial sample set, the shape of  
390 ventral anchor was found to be related to the sampling site in the comparison between Kalemie  
391 2018 and Uvira 2018. In the spatio-temporal sample set, the shape of botch anchors was different  
392 between Mpulungu 2018 and Uvira 2016 (Table S3). The results of RWA (including sliding  
393 landmarks) followed the pattern (Fig. S4).

394 *Effect of host size* - No effect of the host size on the position of specimens was detected in neither  
395 of the presented biplots nor in the linear models for the morphological parameters.

396 In total, just a single morphological character, the length to notch of the dorsal anchor, differed  
397 between the sampling sites in all sample sets. Two additional characters, the branch length of the  
398 ventral bar and the total length of the ventral anchor, differed between the sampling sites in  
399 specimens of *Kapentagyris* spp. collected from *L. miodon*. Finally, the length of the first pair of  
400 marginal hooks differed between the sampling sites for the specimens of *K. tanganicus*  
401 collected from different host species (see 3.1.2.). For further details see Table S2.

### 402 3.2. Genetic diversity

403 The number of polymorphic sites in COI found per monogenean species was 18 (N = 51) for *K.*  
404 *limnotrissae* and 68 (N = 140) for *K. tanganicus*. Both clupeids had a similar number of

405 polymorphic sites, 45 (N = 69) in *L. miodon* and 48 (N = 96) in *S. tanganyicae*, in the COI gene.  
406 Similar levels of nucleotide and haplotype diversity were observed between the two parasite  
407 species and one of the host species: *S. tanganyicae*. Lower genetic diversity was observed for *K.*  
408 *tanganyicanus* when only individuals collected from *S. tanganyicae* were included. The other host  
409 species, *L. miodon*, had higher genetic diversity than both species of *Kapentagyryus* (Table 2).

### 410 3.3. Parasite population genetics

411 First, there was no evident clustering of *K. tanganyicanus* according to host species (see Fig. 5A).  
412 However, significant  $F_{ST}$  value were found between *K. tanganyicanus* infecting different host  
413 species collected in Uvira 2016 ( $F_{ST} = 0.0668$ ;  $P = 0.0112$ ). Haplotype networks indicated neither  
414 geographic, nor school-related structure in either of the monogenean species. All networks  
415 showed a star-like topology with a single dominant haplotype (see Fig. 5B-D). Satellite haplotypes  
416 were mostly separated by a single mutation from the central haplotypes. Significant  $F_{ST}$  values  
417 were also recorded in *K. tanganyicanus* ex *L. miodon* between several sampling sites on a temporal  
418 scale (see enclosed table in Fig. 5). AMOVA calculated for *K. tanganyicanus* ex *L. miodon* showed  
419 that most of the variation was present within populations (96.85%) in comparison to 1.67% among  
420 populations within subbasins and 1.47% among subbasins.

### 421 3.4. Demographic history

422 Signatures of population expansion were detected in both monogenean species and their host  
423 species. Recent population growth was suggested by significantly negative values of Fu's  $F_s$  in *K.*  
424 *limnotrissae* (-20.98;  $P < 0.001$ ), in *K. tanganyicanus* (-27.90;  $P < 0.001$ ), in *L. miodon* (24.09;  $P <$   
425 0.001) and in *S. tanganyicae* (-61.64;  $P < 0.001$ ) as well as Tajima's D in *K. limnotrissae* (-2.48;  $P <$   
426 0.001), in *K. tanganyicanus* (-2.41;  $P < 0.001$ ) and in *S. tanganyicae* (-2.41;  $P < 0.001$ ). In *L. miodon*,  
427 the value of Tajima's D was negative (-1.31) but not significant ( $P = 0.06$ ).

428 The unimodal mismatch distribution was well supported by a non-significant SSD and  $rg$ , indicating  
429 recent population expansion in both *Kapentagyris* species (see Fig. 6A, B). Mismatch analyses  
430 dated the onset of population expansion to 11.8 KYA in *K. limnotrissae* (95% CI: 6.5–16.8 KYA) and  
431 to 17.6 KYA in *K. tanganicanus* (95% CI: 3.3–30.1 KYA).

432 Based on Bayesian Skyline Plot analysis, the start of population growth for *K. tanganicanus* was  
433 estimated around 12 KYA (see Fig. 6D) and the time to the most recent common ancestor (TMRCA)  
434 around 70.9 KYA (95% HDP: 15.6–143.1 KYA). Due to the insufficient number of haplotypes, BSP  
435 could not track past changes of effective population size back to more than 7 KYA in the case of *K.*  
436 *limnotrissae* (see Fig. 6C). No sign of population growth was observed and the TMRCA was  
437 estimated at 14.4 KYA (95% HDP: 6.5–24.1 KYA).

### 438 3.5. Nuclear-mitochondrial discordance

439 Based on the comparison of rDNA markers published in Kmentová et al. (2018) and the obtained  
440 COI sequences of the same specimens, nuclear–mitochondrial discordance was documented for  
441 four individuals of *Kapentagyris* collected from *L. miodon* (see Fig. 5A). For two of these four  
442 cases, morphological vouchers are available (specimens on slides deposited under X.4.04 and  
443 XI.1.20 in HU). Their morphology and haplotype of 28S and/or 18S and ITS-1 rDNA (MK521656–59  
444 and MK521661–64) are characteristic for *K. limnotrissae*, whereas the mitochondrial COI  
445 haplotype is that of *K. tanganicanus*.

## 446 Discussion

447 The geographic and temporal population structure, and demographic history of two monogenean  
448 species of *Kapentagyris* infecting clupeid hosts in Lake Tanganyika were investigated. Although,  
449 morphological comparison of the parasites' sclerotised structures did not show clear patterns of  
450 differentiation along a north-south axis, significant differences between some of them indicate

451 spatio-temporal differentiation. Moreover, molecular analyses suggest a weak geographic  
452 population structure with some temporal differentiation. Finally, both species of *Kapentagyris*  
453 showed a similar pattern of recent population expansion, presumably correlated with Pleistocene  
454 climate change and subsequent lake-level fluctuations.

455 *Monogeneans as tags for the geographical population structure of clupeids*

456 The pelagic environment, promoting dispersal, and the large effective population size constrain  
457 genetic drift and differentiation in pelagic fishes (Gonzalez and Zardoya, 2007; Koblmüller et al.,  
458 2019; Martínez et al., 2006). Moreover, the patchy production of phytoplankton in Lake  
459 Tanganyika may promote seasonal migration following the prey and population mixing in pelagic  
460 fishes (Phiri and Shirakihara, 1999; Plisnier et al., 2009; van Zwieten et al., 2002). On the other  
461 hand, population differentiation in the pelagic realm might be facilitated by the presence of  
462 physical barriers such as currents (Podsetchine and Huttula, 2000) or geographical distance  
463 (Gonzalez and Zardoya, 2007). Although the migration patterns of clupeids have not been resolved  
464 yet, some isolation by distance along a north-south gradient was detected, suggesting limits to  
465 lake-wide migration in *S. tanganyicae* (De Keyzer et al., 2019). This was also seen in the chemical  
466 composition of otoliths in both species (Sako et al., 2005).

467 *Morphological variation* - Based on our comprehensive study, morphometrics of monogenean  
468 haptoral and male copulatory organ structures showed in some cases significant intraspecific  
469 shape variation with respect to sampling site. However, none of the approaches used identified a  
470 morphological character that was unambiguously specific to a particular sampling site in neither of  
471 the various sample sets. Interestingly, even though the shape of both anchors mirrored the  
472 pattern of the overall haptoral morphology, the detailed morphology of neither of these  
473 structures provided sufficient resolution to resolve the geographic origin of a monogenean  
474 individual. Significantly different morphological characters between the sampling sites in 2016

475 were not found between the specimens from the same localities in 2018. This suggests  
476 dependency of phenotypic differentiation on environmental conditions rather than fidelity to a  
477 geographic location in *Kapentagyryus* spp. and consequently of their clupeid host species.  
478 Temperature (Brazenor et al., 2018; Dávidová et al., 2005; Ergens and Gelnar, 1985; Mo, 1993),  
479 pollutants (Beaumont, 1997) or other environmental factors (Cable and Harris, 2002; Olstad et al.,  
480 2009) influence the morphology of monogeneans. The morphological differences of *Kapentagyryus*  
481 spp. observed between some of the sampling sites might hence be attributed to environmental  
482 factors directly influencing the parasites' morphology or indirectly through host morphology.  
483 These may induce geographical patterns via restricted host - parasite migration, or via similar  
484 environmental conditions in geographically isolated locations. This might explain the clustering of  
485 geographically isolated specimens of *K. tanganicanus* from Mpulungu and Kalemie (Fig. 3A).  
486 Interestingly, spatio-temporal variation in sample sets of fresh supported the hypothesis of  
487 environmentally-dependent variation, specific to site and time. In Lake Tanganyika, geographical  
488 and seasonal variation in thermal stratification, the level of oxygen (Hecky et al., 1978; Langenberg  
489 et al., 2002), pH (Plisnier et al., 1999), chemical (Degens et al., 1971), phytoplankton composition  
490 (Descy et al., 2005) and algal succession (Agawin et al., 2000) have been reported. They are driven  
491 mostly by wind conditions (Hecky et al., 1978; Langenberg et al., 2003). However, no experimental  
492 data for representatives of *Kapentagyryus* are currently available to attribute observed  
493 morphological differentiation to specific environmental factor.

494 *Different host, different story* - Interestingly, the number of morphometric characters related to  
495 sampling site differed between the sample sets. While a maximum of two characters was  
496 informative in the case of *K. limnotrissae*, a species specific to *L. miodon*, this number was  
497 considerably higher in *K. tanganicanus* collected from the same host species. Clupeids form size-  
498 dependent schools (Misund, 1993). Host-size dependent intensity of infection between

499 *Kapentagyris* spp. collected from *L. miodon* was observed (*K. limnotrissae* being more prevalent  
500 on smaller *L. miodon* and vice versa, own unpublished results). Therefore, observed discrepancy in  
501 differentiation between species of *Kapentagyris* might be explained by a difference in migration  
502 capacity between fish schools (Nøttestad et al., 1999). Moreover, the number of significantly  
503 different morphological characters between the groups of *K. tanganicus* ex *S. tanganicae* was  
504 lower compared to the individuals collected from *L. miodon*. Such a pattern might be related to  
505 the difference in ecology between the host species as *S. tanganicae* displays more pelagic life style  
506 compared to *L. miodon* (Mannini et al., 1996; Mulimbwa and Mannini, 1993). However, this result  
507 might also be influenced by the small number of specimens collected from *S. tanganicae*.

508 *Genetic population structure* - Generally, the genetic structure of parasites is strongly connected  
509 with the dispersal capacity of their hosts (Miura et al., 2006) and their reproductive mode,  
510 generation time and population size. The COI-based median joining networks of both monogenean  
511 species exhibited comparable core-satellite topologies with similar levels of variation in haplotype  
512 and nucleotide diversity. Given that no clear geographical structure appeared from the haplotype  
513 network of none of the three monogenean/host species combinations, we suggest geographical  
514 panmixia with temporal effects in both species of monogeneans infecting Lake Tanganyika  
515 clupeids. This result corresponds with the general biology of clupeids, with assumed lake-wide  
516 migration patterns (De Keyzer et al., 2019; Hauser et al., 1998; Junker et al., 2019; Mulimbwa and  
517 Shirakihara, 1994). In general, studies conducted on marine clupeids do not show strong  
518 population structure, neither using genetic markers (García-Rodríguez et al., 2011; Gonzalez and  
519 Zardoya, 2007; Kinsey et al., 1994) nor fish tags (Clark, 1945). Nevertheless, and despite the shared  
520 COI haplotypes, significant genetic divergence among some of the pre-defined populations of *K.*  
521 *tanganicus* from *L. miodon* was detected based on  $F_{ST}$ . Such temporal genetic structure without  
522 clear evidence for a geographical pattern could be explained by restricted migration of clupeid



523 hosts, random genetic drift across generations or cohorts related to overfishing of declining  
524 clupeid populations in the lake (Mölsä et al., 1999) or recruitment-dependent population  
525 fluctuations in r-strategic fish stocks (Watanabe et al., 1995). Interestingly, a recent study by  
526 Junker et al. (2019) suggested that population structure in *L. miodon* is linked to chromosomal  
527 inversions. Notably, genetic diversity of *K. tanganicus* in COI is comparable to its host: *S.*  
528 *tanganicae*. However, when only parasite individuals collected from this host species were  
529 included, the value was lower. Nucleotide diversity in *L. miodon* is much higher than in both  
530 species of *Kapentagyris* (see Table 2). The level of genetic variation and impact of genetic drift  
531 depends on effective population size (Nei and Tajima, 1981). Given the observed variability in  
532 prevalence and infection intensity of *Kapentagyris* spp. (see Table 1), it is hard to estimate  
533 population size relative to their clupeid hosts and subsequently evaluate the effect of host  
534 population fluctuations. However, no temporal differentiation was observed in neither of the  
535 clupeid hosts so far (De Keyzer et al., 2019; Junker et al., 2019). The reported genetic divergence  
536 of *K. tanganicus* among pre-defined geographical populations can be influenced by stochasticity  
537 related to the small sample size and short fragment length rather than persisting gene flow  
538 barriers. Moreover, the generally reported short generation time of less than a month in  
539 dactylogyrid monogeneans (Harris, 1983; Scott and Nokes, 1984; Xiaoqin et al., 2000). Indeed,  
540 multiple spawning events per year were reported for both species of Tanganyika clupeids  
541 (Mulimbwa and Shirakihara, 1994). Together with their short life span, this may erase the  
542 expected effect of a faster molecular evolution in parasites. Alternatively, monogean  
543 reproduction in the pelagic habitat connected with planktonic larval dispersal might cause  
544 differences in local genetic diversity of parasites. This is known as fluctuating genetic patchiness  
545 (Hellberg et al., 2002). A similar mechanism was suggested for populations of several monogean  
546 species infecting pelagic fish hosts along the coast of China (Li et al., 2011; Shi et al., 2014; Wang  
547 et al., 2016; Yan et al., 2016).

548 We need to know more about the population dynamics of the hosts and parasites to identify the  
549 cause of the mosaic population structure revealed in this study. In order to further evaluate the  
550 magnifying potential of *Kapentagyris* spp., genome-wide markers need to be applied and  
551 compared with similar data on the host species as this study is limited by the single genetic marker  
552 being used. A promising approach to clarify the true nature of the interaction between  
553 environment, host and parasite are waterscape genomic and transcriptomic studies (Grummer et  
554 al., 2019). Here, the peculiarities of the aquatic environment are taken in consideration in the  
555 analysis of populations. Promising examples are the highly resolved population structure of well-  
556 dispersing taxa (Clucas et al., 2018) and dual transcriptomic studies in host and parasite (Feis et al.,  
557 2018).

#### 558 *Parasite diversification in the pelagic zone of Lake Tanganyika*

559 The core-satellite structure of the haplotype networks and the lower haplotype and nucleotide  
560 diversity in comparison to *Cichlidogyrus casuarinus* Pariselle, Muterezi Bukinga & Vanhove, 2015, a  
561 monogenean species infecting bathybatine benthopelagic cichlids in Lake Tanganyika (Kmentová  
562 et al., 2016; Pariselle et al., 2015) points to more recent diversification in both species of  
563 *Kapentagyris*. This might be attributed to limited allopatric divergence in view of a higher  
564 dispersal capacity and larger population densities of clupeids in Lake Tanganyika compared to  
565 pelagic cichlid species (Coulter, 1991; Koblmüller et al., 2019, 2015).

566 Interestingly, morphological differentiation of *K. tanganicanus*, influenced by the host species and  
567 detected in a previous study (Kmentová et al., 2018), was supported by genetic differentiation of  
568 the specimens sampled off Uvira in 2016. Our results indicate genetic differentiation of *K.*  
569 *tanganicanus* with respect to the clupeid host species. Most probably it happened after a recent  
570 host switch. However, given the uniformity in three nuclear gene fragments, the low  $F_{ST}$  value and  
571 the many shared COI haplotypes of *K. tanganicanus* collected from different host species, we

572 hypothesize that speciation is prevented as hosts occupy the same environment and have a prey-  
573 predator relationship between them (Coulter, 1991; Mulimbwa and Shirakihara, 1994), which has  
574 been proposed to be linked to host sharing in monogeneans (Strona, 2015). This should be further  
575 verified by genetic characterisation of more individuals combined with genome wide data. The  
576 results fit the scenario of a relatively low rate of intraspecific divergence in barrier-free pelagic  
577 compared to littoral fish species (Kmentová et al., 2016; Koblmüller et al., 2019, 2015).

#### 578 *Demographic history*

579 Haplotype structure pointed to a recent population expansion for both species of *Kapentagyryrus*  
580 and their clupeid hosts. The time of the onset of population growth inferred for *K. tanganicanus*  
581 corresponded with global climate changes and subsequent lake level rise. Indeed, 10 KYA is the  
582 estimated end of the last Little Ice Age, which corresponds with the end of a dry period in East  
583 Africa (McGlue et al., 2008). Sea level changes and climate oscillations have measurably influenced  
584 the demographic history of monogeneans (Wang et al., 2016; Yan et al., 2016). We suggest that  
585 expansion and population growth of *Kapentagyryrus* spp. are linked to rising lake levels. We assume  
586 that such patterns might be also found in the clupeid host species as climate induced lake level  
587 fluctuations have also influenced the demographic history of eupelagic bathybatine cichlids  
588 (Koblmüller et al., 2019) and their monogenean parasite *C. casuarinus* (Kmentová et al., 2016). The  
589 onset of population expansion and the time to the most recent common ancestor was estimated  
590 for both species of *Kapentagyryrus* to have been more recent than for *C. casuarinus* (using the same  
591 substitution rate). Possible explanations for this difference could be the different life-style and  
592 population size of the hosts, host range of the parasites and difference in substitution rates.

#### 593 *Nuclear–mitochondrial discordance*

594 The mitochondrial haplotype of *K. tanganicanus* was detected in four specimens identified as *K.*  
595 *limnotrissae*. We interpret this as evidence for mitochondrial introgression of *K. tanganicanus* into

596 *K. limnotrissae*. All four individuals were homozygous at all three nuclear loci analysed and  
597 identical to other individuals of *K. limnotrissae*, which excludes that they are F1 hybrids of  
598 *Kapentagyryus* spp. Given the broader host range of *K. tanganicus* compared to its congener, the  
599 introgression might result from a recent host switch and a demographic expansion of *K.*  
600 *tanganicus* (Barson et al., 2010; Rieseberg et al., 2007; Seixas et al., 2018). However, our data  
601 does not allow unambiguous differentiation among incomplete lineage sorting, introgression, or  
602 contemporary hybridisation. Nevertheless, as no intermediate nuclear haplotype was captured,  
603 the presence of a mitochondrial genome of one species in the nuclear environment of another  
604 species suggests mitochondrial introgression followed by recurrent backcrossing into the paternal  
605 species. Eventually, the introgression resulted in dilution and loss of alleles inherited from the  
606 maternal species (Okamoto et al., 2010). A hybridisation event would support the above-  
607 mentioned scenario of a recent host switch of *K. tanganicus* followed by temporal  
608 differentiation of infection related to host size (own unpublished data). Moreover, the apparent  
609 morphological similarity in the male copulatory organ of the two parasite species contradicts the  
610 scenario of intrahost speciation (Jarkovský et al., 2004). Although hybridisation has been reported  
611 in gyrodactylid monogeneans (Barson et al., 2010; Schelkle et al., 2012), this is the first case for  
612 dactylogyrid monogeneans. The poor documentation of hybridisation in monogeneans might be  
613 related to the lack of studies combining morphology, nuclear and mitochondrial markers. In  
614 general, hybridisation is considered a major driver of evolution (Franssen et al., 2015; Hedrick,  
615 2013; Huyse et al., 2013; King et al., 2015) which also impacts the host range of parasites (Henrich  
616 et al., 2013; Huyse et al., 2009).

### 617 *Conclusion*

618 In conclusion, no consistent geographical structure along a north-south axis in neither  
619 *Kapentagyryus* spp. was found (distance between the two most extreme sampling sites is > 600

620 km), suggesting ongoing gene flow throughout Lake Tanganyika. Therefore, our results correspond  
621 with a pattern of weak to no lake-wide population structure of both host species (De Keyzer et al.,  
622 2019; Junker et al., 2019). Temporal structure in some morphological characters might be  
623 attributed to similar environmental conditions in geographically isolated sampling sites, in  
624 combination with restricted host migration. Moreover, significant genetic differentiation was  
625 found between some of the parasite populations. Serial sampling and genomic data should  
626 increase spatio-temporal resolution to track host migration. Some evidence for incipient  
627 speciation in *K. tanganicus* according to host species was found based on mitochondrial data,  
628 despite uniformity in nuclear gene portions. Our findings provide additional support for the impact  
629 of historical lake level changes also on organisms inhabiting the lake's pelagic zone. Finally,  
630 mitonuclear discordance suggests past hybridisation between the two species of *Kapentagyryus*,  
631 which is the first documented case of hybridisation in dactylogyrid monogeneans.

## 632 **Acknowledgments**

633 The authors would like to thank to L. Raisingerová, C. Rahmouni, H. Zimmermann, A. P. H. Bose  
634 and W. Salzburger for help with collecting host samples. M. Jorissen is gratefully acknowledged for  
635 fruitful discussions about monogenean morphological variability and help in the lab. Special thanks  
636 to the staff of the parasitological group at Masaryk University, Brno (Czech Republic), the Research  
637 Group Zoology at Hasselt University (Belgium), Research Centre of Hydrobiology in Uvira (DR  
638 Congo) and Fisheries Research Unit in Mpulungu (Zambia) for their hospitality.

## 639 **Funding**

640 Research has been supported by the Czech Science Foundation (P505/12/G112 (ECIP) and GA19-  
641 13573S), EMBRC Belgium - FWO project GOH3817N as well as by a joint program between the  
642 Austrian agency for international mobility and cooperation in education, science and research and  
643 the Ministry of Education, Youth and Sports (project number 8J18AT007), the Austrian Agency for

644 International Cooperation in Education and Research (OEAD; project number CZ 08/2018; to SK).  
645 MPMV was co-financed by institutional funding of the Finnish Museum of Natural History and the  
646 Belgian Directorate-General for Development Cooperation and Humanitarian Aid (CEBioS  
647 program). ELRDk was supported by the Belgian Development Cooperation through VLIR-UOS  
648 (VLADOC scholarship NDOC2016PR006 to ELRDk and South Initiative project CD2018SIN218A101).  
649 Fieldwork was carried out with the approval of the competent local authorities under mission  
650 statement 031/MINRST/CRH-U/2016 and the permission of the Fisheries Department of Zambia  
651 and under a study permit issued by the government of Zambia (SP 008732).

652

## 653 **References**

- 654 Agawin, N.S.R., Duarte, C.M., Agustí, S., 2000. Nutrient and temperature control of the  
655 contribution of picoplankton to phytoplankton biomass and production. *Limnol. Oceanogr.*  
656 45, 591–600. <https://doi.org/10.4319/lo.2000.45.3.0591>
- 657 Baldwin, R.E., Banks, M.A., Jacobson, K.C., 2012. Integrating fish and parasite data as a holistic  
658 solution for identifying the elusive stock structure of Pacific sardines (*Sardinops sagax*). *Rev.*  
659 *Fish Biol. Fish.* 22, 137–156. <https://doi.org/10.1007/s11160-011-9227-5>
- 660 Barson, M., Přikrylová, I., Vanhove, M.P.M., Huyse, T., 2010. Parasite hybridization in African  
661 *Macrogyrodactylus* spp. (Monogenea, Platyhelminthes) signals historical host distribution.  
662 *Parasitology* 137, 1585–1595. <https://doi.org/10.1017/S0031182010000302>
- 663 Beaumont, M., 1997. Book review: Sublethal and chronic effects of pollutants on freshwater fish,  
664 edited by R. Müller and R. Lloyd. *Regul. Rivers Res. Manag.* 13, 95–96.  
665 [https://doi.org/10.1002/\(SICI\)1099-1646\(199701\)13:1<95::AID-RRR428>3.0.CO;2-V](https://doi.org/10.1002/(SICI)1099-1646(199701)13:1<95::AID-RRR428>3.0.CO;2-V)
- 666 Brazenor, A.K., Saunders, R.J., Miller, T.L., Hutson, K.S., 2018. Morphological variation in the

667 cosmopolitan fish parasite *Neobenedenia girellae* (Capsalidae: Monogenea). Int. J. Parasitol.  
668 48, 125–134. <https://doi.org/10.1016/J.IJPARA.2017.07.009>

669 Cable, J., Harris, P.D., 2002. Gyrodactylid developmental biology: historical review, current status  
670 and future trends. Int. J. Parasitol. 32, 255–80.

671 Catalano, S.R., Whittington, I.D., Donnellan, S.C., Gillanders, B.M., 2014. Parasites as biological tags  
672 to assess host population structure: Guidelines, recent genetic advances and comments on a  
673 holistic approach. Int. J. Parasitol. Parasites Wildl. 3, 220–6.  
674 <https://doi.org/10.1016/j.ijppaw.2013.11.001>

675 Clark, F.N., 1945. Results of tagging experiments in California on Sardine (*Sardinops caerulea*). Fish.  
676 Bull. 61, 93.

677 Clucas, G. V., Younger, J.L., Kao, D., Emmerson, L., Southwell, C., Wienecke, B., Rogers, A.D., Bost,  
678 C.A., Miller, G.D., Polito, M.J., Lelliott, P., Handley, J., Crofts, S., Phillips, R.A., Dunn, M.J.,  
679 Miller, K.J., Hart, T., 2018. Comparative population genomics reveals key barriers to dispersal  
680 in Southern Ocean penguins. Mol. Ecol. 27, 4680–4697. <https://doi.org/10.1111/mec.14896>

681 Coulter, G.W., 1991. Pelagic Fish, in: Coulter, G.W. (Ed.), Lake Tanganyika and Its Life. Natural  
682 History Museum & Oxford University Press, London Oxford & New York, pp. 111–150.

683 Cox, C.F., Cox, M.A.A., 1989. Procrustes analysis, in: Cox, C.F., Cox, M.A.A. (Eds.), Multidimensional  
684 Scaling. Second Edition. Chapman & Hall, London, pp. 123–139.  
685 <https://doi.org/10.1137/1028043>

686 Dag, O., Dolgun, A., Konar, N.M., 2018. onewaytests: an R package for one-way tests in  
687 independent groups designs. R J. 10, 175–199. <https://doi.org/doi.org/10.32614/RJ-2018-022>

688 Danley, P.D., Husemann, M., Ding, B., Dipietro, L.M., Beverly, E.J., Peppe, D.J., 2012. The impact of

689 the geologic history and paleoclimate on the diversification of East African cichlids. *Int. J. Evol.*  
690 *Biol.* 574851. <https://doi.org/10.1155/2012/574851>

691 Dávidová, M., Jarkovský, J., Matějusková, I., Gelnar, M., 2005. Seasonal occurrence and metrical  
692 variability of *Gyrodactylus rhodei* Žitňan 1964 (Monogenea, Gyrodactylidae). *Parasitol. Res.*  
693 95, 398–405. <https://doi.org/10.1007/s00436-005-1311-0>

694 De Keyzer, E.L.R., De Corte, Z., Van Steenberge, M., Raeymaekers, J.A.M., Calboli, F.C.F.,  
695 Kmentová, N., N'Sibula Mulimbwa, T., Virgilio, M., Vangestel, C., Mulungula, P.M., Volckaert,  
696 F.A.M., Vanhove, M.P.M., 2019. First genomic study on Lake Tanganyika sprat *Stolothrissa*  
697 *tanganicae*: a lack of population structure calls for integrated management of this important  
698 fisheries target species. *BMC Evol. Biol.* 19, 6. <https://doi.org/10.1186/s12862-018-1325-8>

699 Degens, E.T., Von Herzen, R.P., Wong, H.-K., 1971. Lake Tanganyika: Water chemistry, sediments,  
700 geological structure. *Naturwissenschaften* 58, 229–241. <https://doi.org/10.1007/BF00602986>

701 Descy, J.P., Hardy, M.A., Sténuite, S., Pirlot, S., Leporcq, B., Kimirei, I., Sekadende, B., Mwaitega,  
702 S.R., Sinyenza, D., 2005. Phytoplankton pigments and community composition in Lake  
703 Tanganyika. *Freshw. Biol.* 50, 668–684. <https://doi.org/10.1111/j.1365-2427.2005.01358.x>

704 Drummond, A.J., Rambaut, A., Shapiro, B., Pybus, O.G., 2005. Bayesian coalescent inference of  
705 past population dynamics from molecular sequences. *Mol. Biol. Evol.* 22, 1185–1192.  
706 <https://doi.org/10.1093/molbev/msi103>

707 Edgar, R.C., 2004. MUSCLE: Multiple sequence alignment with high accuracy and high throughput.  
708 *Nucleic Acids Res.* 32, 1792–1797. <https://doi.org/10.1093/nar/gkh340>

709 Emmett, R.L., Brodeur, R.D., Miller, T.D., Pool, S.S., Krutzikowsky, G.K., Bentley, P.J., Mccrae, J.,  
710 2005. Pacific sardine (*Sardinops sagax*) abundance, distribution, and ecological relationships  
711 in the Pacific Northwest. *Calif. Coop. Ocean. Fish. Investig. Rep.* 46, 122–143.



712 Ergens, R., Gelnar, M., 1985. Experimental verification of the effect of temperature on the size of  
713 the hard parts of haptor of *Gyrodactylus katharineri* Malberg 1964. *Folia Parasitol. (Praha)*.  
714 32, 377–380.

715 Excoffier, L., Lischer, H.E.L., 2010. Arlequin suite ver 3.5: a new series of programs to perform  
716 population genetics analyses under Linux and Windows. *Mol. Ecol. Resour.* 10, 564–567.  
717 <https://doi.org/10.1111/j.1755-0998.2010.02847.x>

718 Feis, M.E., John, U., Lokmer, A., Luttikhuisen, P.C., Wegner, K.M., 2018. Dual transcriptomics  
719 reveals co-evolutionary mechanisms of intestinal parasite infections in blue mussels *Mytilus*  
720 *edulis*. *Mol. Ecol.* 27, 1505–1519. <https://doi.org/10.1111/mec.14541>

721 Folmer, O., Black, M., Hoeh, W., Lutz, R., Vrijenhoek, R., 1994. DNA primers for amplification of  
722 mitochondrial cytochrome c oxidase subunit I from diverse metazoan invertebrates. *Mol.*  
723 *Mar. Biol. Biotechnol.* 3, 294–299. <https://doi.org/10.1071/ZO9660275>

724 Fox, J., Weisberg, S., 2011. An {R} companion to applied regression, Second. ed. Sage, Thousand  
725 Oaks {CA}.

726 Franssen, F., Bilska-Zajac, E., Deksne, G., Sprong, H., Pozio, E., Rosenthal, B., Rozycki, M., van der  
727 Giessen, J., 2015. Genetic evidence of interspecies introgression of mitochondrial genomes  
728 between *Trichinella spiralis* and *Trichinella britovi* under natural conditions. *Infect. Genet.*  
729 *Evol.* 36, 323–332. <https://doi.org/10.1016/J.MEEGID.2015.10.005>

730 Fu, Y.X., 1997. Statistical tests of neutrality of mutations against population growth, hitchhiking  
731 and background selection. *Genetics* 147, 915–25.

732 García-Rodríguez, F.J., García-Gasca, S.A., Cruz-Agüero, J.D. La, Cota-Gómez, V.M., 2011. A study of  
733 the population structure of the Pacific sardine *Sardinops sagax* (Jenyns, 1842) in Mexico  
734 based on morphometric and genetic analyses. *Fish. Res.* 107, 169–176.

735 <https://doi.org/10.1016/J.FISHRES.2010.11.002>

736 Gonzalez, E.G., Zardoya, R., 2007. Relative role of life-history traits and historical factors in shaping  
737 genetic population structure of sardines (*Sardina pilchardus*). BMC Evol. Biol. 7, 197.  
738 <https://doi.org/10.1186/1471-2148-7-197>

739 Grummer, J.A., Beheregaray, L.B., Bernatchez, L., Hand, B.K., Luikart, G., Narum, S.R., Taylor, E.B.,  
740 2019. Aquatic landscape genomics and environmental effects on genetic variation. Trends  
741 Ecol. Evol. <https://doi.org/10.1016/j.tree.2019.02.013>

742 Handy, S.M., Deeds, J.R., Ivanova, N. V., Hebert, P.D.N., Hanner, R.H., Ormos, A., Weigt, L.A.,  
743 Moore, M.M., Yancy, H.F., 2011. A single-laboratory validated method for the generation of  
744 DNA barcodes for the identification of fish for regulatory compliance. J. AOAC Int. 94, 201–  
745 210.

746 Harris, P.D., 1983. The morphology and life-cycle of the oviparous *Oögyrodactylus farlowellae* gen.  
747 et sp.nov. (Monogenea, Gyrodactylidea). Parasitology 87, 405–420.  
748 <https://doi.org/10.1017/S0031182000082937>

749 Hauser, L., Carvalho, G.R., Pitcher, T.J., 1998. Genetic population structure in the Lake Tanganyika  
750 sardine *Limnothrissa miodon*. J. Fish Biol. 53, 413–429. [https://doi.org/10.1111/j.1095-](https://doi.org/10.1111/j.1095-8649.1998.tb01040.x)  
751 [8649.1998.tb01040.x](https://doi.org/10.1111/j.1095-8649.1998.tb01040.x)

752 Hecky, R.E., Fee, E.J., Kling, H., Rudd, J.W.M., 1978. Studies on the planktonic ecology of Lake  
753 Tanganyika. Winnipeg, Man.: Fisheries and Marine Service.

754 Hedrick, P.W., 2013. Adaptive introgression in animals: examples and comparison to new mutation  
755 and standing variation as sources of adaptive variation. Mol. Ecol. 22, 4606–4618.  
756 <https://doi.org/10.1111/mec.12415>

757 Hellberg, M.E., Burton, R.S., Neigel, J.E., Palumbi, S.R., 2002. Genetic assessment of connectivity  
758 among marine populations. *Bull. Mar. Sci.* 70, 273–290.

759 Henrich, T., Benesh, D.P., Kalbe, M., 2013. Hybridization between two cestode species and its  
760 consequences for intermediate host range. *Parasit. Vectors* 6, 33.  
761 <https://doi.org/10.1186/1756-3305-6-33>

762 Huyse, T., Van den Broeck, F., Hellemans, B., Volckaert, F.A.M., Polman, K., 2013. Hybridisation  
763 between the two major African schistosome species of humans. *Int. J. Parasitol.* 43, 687–689.  
764 <https://doi.org/10.1016/J.IJPARA.2013.04.001>

765 Huyse, T., Webster, B.L., Geldof, S., Stothard, J.R., Diaw, O.T., Polman, K., Rollinson, D., 2009.  
766 Bidirectional introgressive hybridization between a cattle and human schistosome species.  
767 *PLoS Pathog.* 5, e1000571. <https://doi.org/10.1371/journal.ppat.1000571>

768 James, A.G., Hutchings, L., Brownell, C.L., Horstman, D.A., 1988. Methods of capture and transfer  
769 to the laboratory of wild pelagic fish. *South African J. Mar. Sci.* 6, 17–21.  
770 <https://doi.org/10.2989/025776188784480519>

771 Jarkovský, J., Morand, S., Šimková, A., Gelnar, M., 2004. Reproductive barriers between congeneric  
772 monogenean parasites (*Dactylogyus*: Monogenea): Attachment apparatus morphology or  
773 copulatory organ incompatibility? *Parasitol. Res.* 92, 95–105.  
774 <https://doi.org/10.1007/s00436-003-0993-4>

775 Jombart, T., 2008. Adegnet: A R package for the multivariate analysis of genetic markers.  
776 *Bioinformatics* 24, 1403–1405. <https://doi.org/10.1093/bioinformatics/btn129>

777 Junker, J., Rick, J.A., McIntyre, P.B., Kimirei, I., Sweke, E.A., Mosille, J.B., Werli, B., Dinkel, C.,  
778 Mwaiko, S., Seehausen, O., Wagner, C.E., 2019. Sex differentiation and a chromosomal  
779 inversion lead to cryptic diversity in Lake Tanganyika sardines. *bioRxiv* 800904.

780 <https://doi.org/10.1101/800904>

781 Kassambara, A., Mundt, F., 2017. factoextra: extract and visualize the results of multivariate data  
782 analyses.

783 King, K.C., Stelkens, R.B., Webster, J.P., Smith, D.F., Brockhurst, M.A., 2015. Hybridization in  
784 parasites: consequences for adaptive evolution, pathogenesis, and public health in a changing  
785 w. PLOS Pathog. 11, e1005098. <https://doi.org/10.1371/journal.ppat.1005098>

786 Kinsey, S.T., Orsoy, T., Bert, T.M., Mahmoudi, B., 1994. Population structure of the Spanish sardine  
787 *Sardinella aurita*: natural morphological variation in a genetically homogeneous population.  
788 Mar. Biol. 118, 309–317. <https://doi.org/10.1007/BF00349798>

789 Kirchberger, P.C., Sefc, K.M., Sturmbauer, C., Koblmüller, S., 2012. Evolutionary history of Lake  
790 Tanganyika's predatory deepwater cichlids. Int. J. Evol. Biol. 2012, 716209,  
791 [10.1155/2012/716209](https://doi.org/10.1155/2012/716209). <https://doi.org/10.1155/2012/716209>

792 Klingenberg, C.P., 2011. MORPHOJ: an integrated software package for geometric morphometrics.  
793 Mol. Ecol. Resour. 11, 353–357. <https://doi.org/10.1111/j.1755-0998.2010.02924.x>

794 Klingenberg, C.P., Monteiro, L.R., 2005. Distances and directions in multidimensional shape spaces:  
795 implications for morphometric applications. Syst. Biol. 54, 678–688.  
796 <https://doi.org/10.1080/10635150590947258>

797 Kmentová, N., Gelnar, M., Mendlová, M., Van Steenberge, M., Koblmüller, S., Vanhove, M.P.M.,  
798 2016. Reduced host-specificity in a parasite infecting non-littoral Lake Tanganyika cichlids  
799 evidenced by intraspecific morphological and genetic diversity. Sci. Rep. 6, 39605.  
800 <https://doi.org/10.1038/srep39605>

801 Kmentová, N., Van Steenberge, M., Raeymaekers, J.A.R., Koblmüller, S., Hablützel, P.I., Muterezi

802 Bukinga, F., Mulimbwa N'sibula, T., Masilya Mulungula, P., Nzigidahera, B., Ntakimazi, G.,  
803 Gelnar, M., Vanhove, M.P.M., 2018. Monogenean parasites of sardines in Lake Tanganyika:  
804 diversity, origin and intra-specific variability. *Contrib. to Zool.* 87, 105–132.

805 Koblmüller, S., Odhiambo, E.A., Sinyinza, D., Sturmbauer, C., Sefc, K.M., 2015. Big fish, little  
806 divergence: phylogeography of Lake Tanganyika's giant cichlid, *Boulengerochromis microlepis*.  
807 *Hydrobiologia* 748, 29–38. <https://doi.org/10.1007/s10750-014-1863-z>

808 Koblmüller, S., Zangl, L., Börger, C., Daill, D., Vanhove, M.P.M., Sturmbauer, C., Sefc, K.M., 2019.  
809 Only true pelagics mix: comparative phylogeography of deepwater bathybatine cichlids from  
810 Lake Tanganyika. *Hydrobiologia* 832, 93–103. <https://doi.org/10.1007/s10750-018-3752-3>

811 Kumar, S., Stecher, G., Tamura, K., Gerken, J., Pruesse, E., Quast, C., Schweer, T., Peplies, J.,  
812 Ludwig, W., Glockner, F., 2016. MEGA7: Molecular evolutionary genetics analysis Version 7.0  
813 for bigger datasets. *Mol. Biol. Evol.* 33, 1870–1874. <https://doi.org/10.1093/molbev/msw054>

814 Kurki, H., Vuorinen, I., Bosma, E., Bwebwa, D., 1999. Spatial and temporal changes in copepod  
815 zooplankton communities of Lake Tanganyika, in: Lindqvist, O. V., Molsd, H., Salonen, K.,  
816 Sarvala, J. (Eds.), *From Limnology to Fisheries: Lake Tanganyika and Other Large Lakes*. Kluwer  
817 Academic Publishers., Dordrecht, pp. 105–114. [https://doi.org/10.1007/978-94-017-1622-](https://doi.org/10.1007/978-94-017-1622-2_10)  
818 [2\\_10](https://doi.org/10.1007/978-94-017-1622-2_10)

819 Langenberg, V.T., Mwape, L.M., Tshibangu, K., Tumba, J.-M., Koelmans, A.A., Roijackers, R.,  
820 Salonen, K., Sarvala, J., Mölsä, H., 2002. Comparison of thermal stratification, light  
821 attenuation, and chlorophyll- a dynamics between the ends of Lake Tanganyika. *Aquat.*  
822 *Ecosyst. Health Manag.* 5, 255–265. <https://doi.org/10.1080/14634980290031956>

823 Langenberg, V.T., Sarvala, J., Roijackers, R., 2003. Effect of wind induced water movements on  
824 nutrients, chlorophyll- a, and primary production in Lake Tanganyika. *Aquat. Ecosyst. Health*

825           Manag. 6, 279–288. <https://doi.org/10.1080/14634980301488>

826 Leigh, J.W., Bryant, D., 2015. PopART: full-feature software for haplotype network construction.  
827           Methods Ecol. Evol. 6, 1110–1116.

828 Li, M., Shi, S.F., Brown, C.L., Yang, T.B., 2011. Phylogeographical pattern of *Mazocraeoides*  
829           *gonialosae* (Monogenea, Mazocraeidae) on the dotted gizzard shad, *Konosirus punctatus*,  
830           along the coast of China. Int. J. Parasitol. 41, 1263–1272.  
831           <https://doi.org/10.1016/j.ijpara.2011.07.012>

832 Littlewood, D.T.J., Rohde, K., Clough, K.A., 1997. Parasite speciation within or between host  
833           species? - Phylogenetic evidence from site-specific polystome monogeneans. Int. J. Parasitol.  
834           27, 1289–1297. [https://doi.org/10.1016/S0020-7519\(97\)00086-6](https://doi.org/10.1016/S0020-7519(97)00086-6)

835 Lockyer, A.E., Olson, P.D., Ostergaard, P., Rollinson, D., Johnston, D.A., Attwood, S.W., Southgate,  
836           V.R., Horak, P., Snyder, S.D., Le, T.H., Agatsuma, T., McManus, D.P., Carmichael, A.C., Naem,  
837           S., Littlewood, D.T.J., 2003. The phylogeny of the Schistosomatidae based on three genes with  
838           emphasis on the interrelationships of *Schistosoma* Weinland, 1858. Parasitology 126, 203–24.  
839           <https://doi.org/https://doi.org/10.1017/S0031182002002792>

840 Mannini, P., Aro, E., Katonda, K.I., Kassaka, B., Mambona, C., Milindi, G., Paffen, P., Verburg, P.,  
841           1996. Pelagic fish stocks of Lake Tanganyika: biology and exploitation. FAO/FINNIDA research  
842           for the management of the fisheries of Lake Tanganyika., GCP/RAF/271/FIN—TD/53 (En).  
843           Bujumbura.

844 Marshall, B.E., 1993. Biology of the African clupeid *Limnothrissa miodon* with reference to its small  
845           size in artificial lakes. Rev. Fish Biol. Fish. 3, 17–38. <https://doi.org/10.1007/BF00043296>

846 Martínez, P., González, E.G., Castilho, R., Zardoya, R., 2006. Genetic diversity and historical  
847           demography of Atlantic bigeye tuna (*Thunnus obesus*). Mol. Phylogenet. Evol. 39, 404–416.

848 <https://doi.org/10.1016/j.ympev.2005.07.022>

849 Mattiucci, S., Abaunza, P., Ramadori, L., Nascetti, G., 2004. Genetic identification of *Anisakis* larvae  
850 in European hake from Atlantic and Mediterranean waters for stock recognition. *J. Fish Biol.*  
851 65, 495–510. <https://doi.org/10.1111/j.0022-1112.2004.00465.x>

852 McGlue, M.M., Lezzar, K.E., Cohen, A.S., Russell, J.M., Tiercelin, J.-J., Felton, A.A., Mbede, E.,  
853 Nkotagu, H.H., 2008. Seismic records of late Pleistocene aridity in Lake Tanganyika, tropical  
854 East Africa. *J. Paleolimnol.* 40, 635–653. <https://doi.org/10.1007/s10933-007-9187-x>

855 Meinilä, M., Kuusela, J., Ziętara, M.S., Lumme, J., 2004. Initial steps of speciation by geographic  
856 isolation and host switch in salmonid pathogen *Gyrodactylus salaris* (Monogenea:  
857 Gyrodactylidae). *Int. J. Parasitol.* 34, 515–526. <https://doi.org/10.1016/j.ijpara.2003.12.002>

858 Misund, O., 1993. Dynamics of moving masses: variability in packing density, shape, and size  
859 among herring, sprat, and saithe schools. *ICES J. Mar. Sci.* 50, 145–160.  
860 <https://doi.org/10.1006/jmsc.1993.1016>

861 Miura, O., Torchin, M.E., Kuris, A.M., Hechinger, R.F., Chiba, S., 2006. Introduced cryptic species of  
862 parasites exhibit different invasion pathways. *Proc. Natl. Acad. Sci. U. S. A.* 103, 19818–23.  
863 <https://doi.org/10.1073/pnas.0609603103>

864 Mo, A., 1993. Seasonal variation of haptor hard parts of *Gyrodactylus derjavini* Mikailov 1975  
865 (Monogenea: Gyrodactylidae) on brown trout *Salmo trutta* L. parr and Atlantic salmon *Salmo*  
866 *salar* L. parr in the River Sandviksela, N. *Syst. Parasitol.* 26, 225–231.

867 Mölsä, H., Reynolds, J.E., Coenen, E.J., Lindqvist, O.V., 1999. Fisheries research towards resource  
868 management on Lake Tanganyika. *Hydrobiologia* 407, 1–24.  
869 <https://doi.org/10.1023/A:1003712708969>

870 Mulimbwa, N., Mannini, P., 1993. Demographic characteristics of *Stolothrissa tanganyicae*,  
871 *Limnothrissa miodon* and *Lates stappersii* in the Northwestern (Zairean) waters of Lake  
872 Tanganyika. CIFA Occas. Pap.

873 Mulimbwa, N., Shirakihara, K., 1994. Growth, recruitment and reproduction of sardines  
874 (*Stolothrissa tanganyicae* and *Limnothrissa miodon*) in northwestern Lake Tanganyika. Tropics  
875 4, 57–67. <https://doi.org/10.3759/tropics.4.57>

876 Nei, M., Tajima, F., 1981. Genetic drift and estimation of effective population size. Genetics 98,  
877 625–640.

878 Nevado, B., Mautner, S., Sturmbauer, C., Verheyen, E., 2013. Water-level fluctuations and  
879 metapopulation dynamics as drivers of genetic diversity in populations of three Tanganyikan  
880 cichlid fish species. Mol. Ecol. 22, 3933–3948. <https://doi.org/10.1111/mec.12374>

881 Nieberding, C., Morand, S., Libois, R., Michaux, J.R., 2004. A parasite reveals cryptic  
882 phylogeographic history of its host. Proceedings. Biol. Sci. 271, 2559–68.  
883 <https://doi.org/10.1098/rspb.2004.2930>

884 Nieberding, C.M., Olivieri, I., 2007. Parasites: proxies for host genealogy and ecology? Trends Ecol.  
885 Evol. 22, 156–165. <https://doi.org/10.1016/j.tree.2006.11.012>

886 Nøttestad, L., Giske, J., Holst, J.C., Huse, G., 1999. A length-based hypothesis for feeding  
887 migrations in pelagic fish. Can. J. Fish. Aquat. Sci. 56, 26–34. <https://doi.org/10.1139/f99-222>

888 Okamoto, M., Nakao, M., Blair, D., Anantaphruti, M.T., Waikagul, J., Ito, A., 2010. Evidence of  
889 hybridization between *Taenia saginata* and *Taenia asiatica*. Parasitol. Int. 59, 70–74.  
890 <https://doi.org/10.1016/j.parint.2009.10.007>

891 Olstad, K., Bachmann, L., Bakke, T. a, 2009. Phenotypic plasticity of taxonomic and diagnostic



892 structures in gyrodactylosis-causing flatworms (Monogenea, Platyhelminthes). Parasitology  
893 136, 1305–1315. <https://doi.org/10.1017/S0031182009990680>

894 Ondračková, M., Matějusková, I., Grabowska, J., 2012. Introduction of *Gyrodactylus perccotti*  
895 (Monogenea) into Europe on its invasive fish host, Amur sleeper (*Perccottus glenii*, Dybowski  
896 1877). Helminthologia 49, 21–26. <https://doi.org/10.2478/s11687-012-0004-3>

897 Pariselle, A., Boeger, W.A., Snoeks, J., Bilong Bilong, C.F., Morand, S., Vanhove, M.P.M., 2011. The  
898 monogenean parasite fauna of cichlids: a potential tool for host biogeography. Int. J. Evol.  
899 Biol. 2011, 471480, 10.4061/2011/471480. <https://doi.org/10.4061/2011/471480>

900 Pariselle, A., Muterezi Bukinga, F., Van Steenberge, M., Vanhove, M.P.M., 2015. Ancyrocephalidae  
901 (Monogenea) of Lake Tanganyika: IV: *Cichlidogyrus* parasitizing species of Bathybatini  
902 (Teleostei, Cichlidae): reduced host-specificity in the deepwater realm? Hydrobiologia 748,  
903 99–119. <https://doi.org/10.1007/s10750-014-1975-5>

904 Pettersen, R.A., Mo, T.A., Hansen, H., Vøllestad, L.A., 2015. Genetic population structure of  
905 *Gyrodactylus thymalli* (Monogenea) in a large Norwegian river system. Parasitology 142,  
906 1693–1702. <https://doi.org/10.1017/S003118201500133X>

907 Phiri, H., Shirakihara, K., 1999. Distribution and seasonal movement of pelagic fish in southern  
908 Lake Tanganyika. Fish. Res. 41, 63–71. [https://doi.org/10.1016/S0165-7836\(99\)00008-9](https://doi.org/10.1016/S0165-7836(99)00008-9)

909 Plisnier, P.-D., Chitamwebwa, D., Mwape, L., Tshibangu, K., Langenberg, V., Coenen, E., 1999.  
910 Limnological annual cycle inferred from physical-chemical fluctuations at three stations of  
911 Lake Tanganyika, in: Lindqvist, O.V., Mölsä, H., Salonen, K., Sarvala, J. (Eds.), From Limnology  
912 to Fisheries: Lake Tanganyika and Other Large Lakes. Springer Netherlands, Dordrecht, pp.  
913 45–58. [https://doi.org/10.1007/978-94-017-1622-2\\_4](https://doi.org/10.1007/978-94-017-1622-2_4)

914 Plisnier, P.D., Mgana, H., Kimirei, I., Chande, A., Makasa, L., Chimanga, J., Zulu, F., Cocquyt, C.,

915 Horion, S., Bergamino, N., Naithani, J., Deleersnijder, E., André, L., Descy, J.P., Cornet, Y.,  
916 2009. Limnological variability and pelagic fish abundance (*Stolothrissa tanganicae* and *Lates*  
917 *stappersii*) in Lake Tanganyika. *Hydrobiologia* 625, 117–134. [https://doi.org/10.1007/s10750-](https://doi.org/10.1007/s10750-009-9701-4)  
918 009-9701-4

919 Podsetchine, V., Huttula, T., 2000. Numerical simulation of wind-driven circulation in lake  
920 tanganyika. *Aquat. Ecosyst. Heal. Manag.* 3, 55–64.  
921 <https://doi.org/10.1080/14634980008656991>

922 Poulin, R., 2007. *Evolutionary ecology of parasites*. 2nd ed. Princeton University Press, Princeton,  
923 New Jersey.

924 R Core Team, 2013. *R: A language and environment for statistical computing*. R Foundation for  
925 Statistical Computing, Vienna, Austria.

926 Rambaut, A., Drummond, A.J., Xie, D., Baele, G., Suchard, M.A., 2018. Posterior summarization in  
927 Bayesian phylogenetics using Tracer 1.7. *Syst. Biol* 67, 2.  
928 <https://doi.org/10.1093/sysbio/syy032>

929 Řehulková, E., Mendlová, M., Šimková, A., 2013. Two new species of *Cichlidogyrus* (Monogenea:  
930 Dactylogyridae) parasitizing the gills of African cichlid fishes (Perciformes) from Senegal:  
931 Morphometric and molecular characterization. *Parasitol. Res.* 112, 1399–1410.  
932 <https://doi.org/10.1007/s00436-013-3291-9>

933 Rieseberg, L.H., Kim, S.-C., Randell, R.A., Whitney, K.D., Gross, B.L., Lexer, C., Clay, K., 2007.  
934 Hybridization and the colonization of novel habitats by annual sunflowers. *Genetica* 129,  
935 149–165. <https://doi.org/10.1007/s10709-006-9011-y>

936 Rodríguez-González, A., Míguez-Lozano, R., Llopis-Belenguer, C., Balbuena, J.A., 2015. Phenotypic  
937 plasticity in haptor structures of *Ligophorus cephalii* (Monogenea: Dactylogyridae) on the

938 flathead mullet (*Mugil cephalus*): a geometric morphometric approach. *Int. J. Parasitol.* 45,  
939 295–303. <https://doi.org/10.1016/j.ijpara.2015.01.005>

940 Rohlf, F., 2006. Tpsdig, digitize landmarks and outlines. Version 2.10. Stony Brook, NY: State  
941 University.

942 Rohlf, F.J., 1993. Relative warp analysis and an example of its application to mosquito wings, in:  
943 Marcus, L., Bello, E., Garcia-Valdecasas, A. (Eds.), *Contributions to Morphometrics*. Stony  
944 Brook, NY: State University, New York, pp. 132–158.

945 Sako, A., O'Reilly, C.M., Hannigan, R., Bickford, N., Johnson, R.L., 2005. Variations in otolith  
946 elemental compositions of two clupeid species, *Stolothrissa tanganicae* and *Limnothrissa*  
947 *miodon* in Lake Tanganyika. *Geochemistry Explor. Environ. Anal.* 5, 91–97.  
948 <https://doi.org/10.1144/1467-7873/03-039>

949 Schelkle, B., Faria, P.J., Johnson, M.B., van Oosterhout, C., Cable, J., 2012. Mixed infections and  
950 hybridisation in monogenean parasites. *PLoS One* 7, e39506.  
951 <https://doi.org/10.1371/journal.pone.0039506>

952 Scott, M.E., Nokes, D.J., 1984. Temperature-dependent reproduction and survival of *Gyrodactylus*  
953 *bullatarudis* (Monogenea) on guppies (*Poecilia reticulata*). *Parasitology* 89, 221–228.  
954 <https://doi.org/10.1017/S0031182000001256>

955 Sefc, K., Mattersdorfe, K., Ziegelbecker, A., Neuhüttler, N., Steiner, O., Goessler, W., Koblmüller, S.,  
956 2017. Shifting barriers and phenotypic diversification by hybridization. *Ecol. Lett.* 20, 651–  
957 662.

958 Seixas, F.A., Boursot, P., Melo-Ferreira, J., 2018. The genomic impact of historical hybridization  
959 with massive mitochondrial DNA introgression. *Genome Biol.* 19, 91.  
960 <https://doi.org/10.1186/s13059-018-1471-8>

961 Shaw, P.W., Turner, G.F., Iddid, M.R., Robinson, R.L., Carvalho, G.R., 2000. Genetic population  
962 structure indicates sympatric speciation of Lake Malawi pelagic cichlids. Proc. R. Soc. B Biol.  
963 Sci. 267, 2273–2280. <https://doi.org/10.1098/rspb.2000.1279>

964 Shi, S.-F., Li, M., Yan, S., Wang, M., Yang, C.-P., Lun, Z.-R., Brown, C.L., Yang, T.-B., 2014.  
965 Phylogeography and demographic history of *Gotocotyla sawara* (Monogenea: Gotocotylidae)  
966 on Japanese Spanish mackerel (*Scomberomorus niphonius*) along the coast of China. J.  
967 Parasitol. 100, 85–92. <https://doi.org/10.1645/13-235.1>

968 Strona, G., 2015. The underrated importance of predation in transmission ecology of direct  
969 lifecycle parasites. Oikos 124, 685–690. <https://doi.org/doi:10.1111/oik.01850>

970 Sturmbauer, C., Baric, S., Salzburger, W., Rüber, L., Verheyen, E., 2001. Lake level fluctuations  
971 synchronize genetic divergences of cichlid fishes in African lakes. Mol. Biol. Evol 18, 144–154.

972 Sturmbauer, C., Börger, C., Van Steenberge, M., Koblmüller, S., 2017. A separate lowstand lake at  
973 the northern edge of Lake Tanganyika? Evidence from phylogeographic patterns in the cichlid  
974 genus *Tropheus*. Hydrobiologia 791, 51–68. <https://doi.org/10.1007/s10750-016-2939-8>

975 Suchard, M.A., Lemey, P., Baele, G., Ayres, D.L., Drummond, A.J., Rambaut, A., 2018. Bayesian  
976 phylogenetic and phylodynamic data integration using BEAST 1.10. Virus Evol. 4.  
977 <https://doi.org/10.1093/ve/vey016>

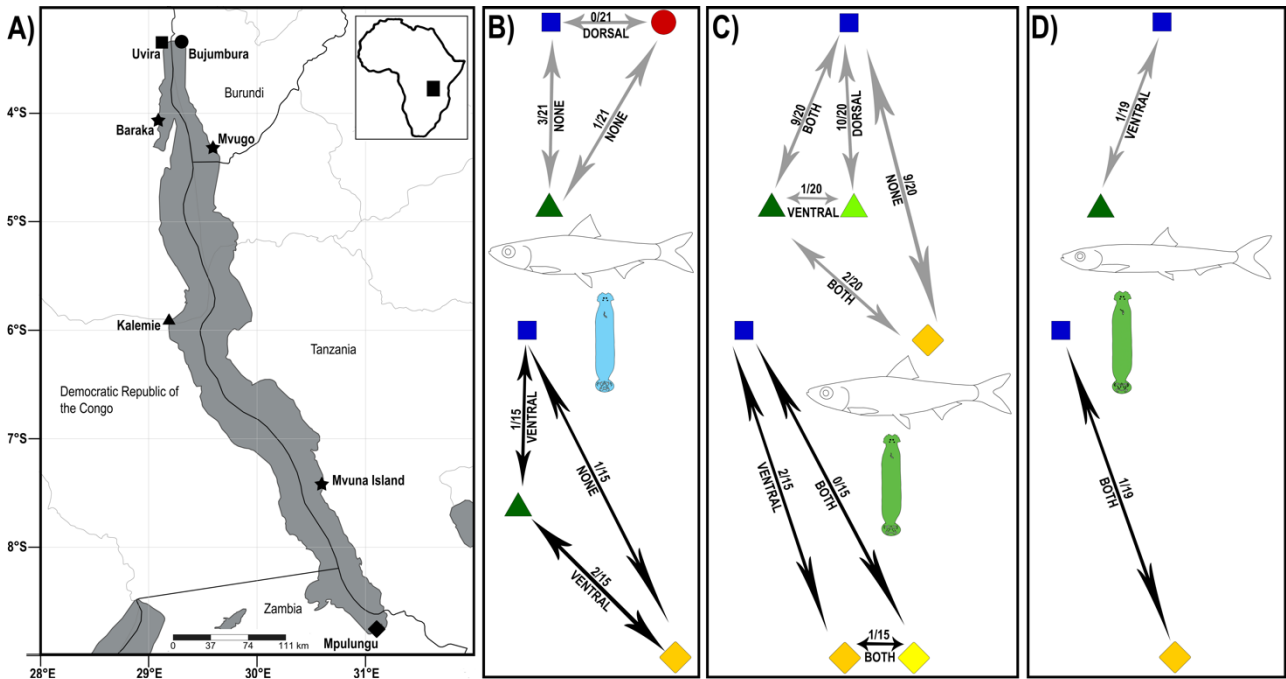
978 Svedäng, H., André, C., Jonsson, P., Elfman, M., Limburg, K.E., 2010. Migratory behaviour and  
979 otolith chemistry suggest fine-scale sub-population structure within a genetically  
980 homogenous Atlantic Cod population. Environ. Biol. Fishes 89, 383–397.  
981 <https://doi.org/10.1007/s10641-010-9669-y>

982 Tajima, F., 1989. Statistical methods to test for nucleotide mutation hypothesis by DNA  
983 polymorphism. Genetics 123, 585–595. <https://doi.org/PMC1203831>

- 984 Tinsley, R.C., 2004. Platyhelminth parasite reproduction: some general principles derived from  
985 monogeneans. *Can. J. Zool.* 82, 270–291. <https://doi.org/10.1139/z03-218>
- 986 van Zwieten, P.A.M., Roest, F.C., Machiels, M.A.M., van Densen, W.L.T., 2002. Effects of inter-  
987 annual variability, seasonality and persistence on the perception of long-term trends in catch  
988 rates of the industrial pelagic purse-seine fishery of northern Lake Tanganyika (Burundi). *Fish.*  
989 *Res.* 54, 329–348. [https://doi.org/10.1016/S0165-7836\(01\)00267-3](https://doi.org/10.1016/S0165-7836(01)00267-3)
- 990 Vignon, M., Pariselle, A., Vanhove, M.P.M., 2011. Modularity in attachment organs of African  
991 *Cichlidogyrus* (Platyhelminthes: Monogenea: Ancyrocephalidae) reflects phylogeny rather  
992 than host specificity or geographic distribution. *Biol. J. Linn. Soc.* 102, 694–706.  
993 <https://doi.org/10.1111/j.1095-8312.2010.01607.x>
- 994 Vilas, R., Criscione, C.D., Blouin, M.S., 2005. A comparison between mitochondrial DNA and the  
995 ribosomal internal transcribed regions in prospecting for cryptic species of platyhelminth  
996 parasites. *Parasitology* 131, 839. <https://doi.org/10.1017/S0031182005008437>
- 997 Wang, M., Yan, S., Brown, C.L., Shaharom-harrison, F., Shi, S., Yang, T., 2016. Phylogeography of  
998 *Tetrancistrum nebulosi* (Monogenea, Dactylogyridae) on the host of mottled spinefoot  
999 (*Siganus fuscescens*) in the South China Sea, inferred from mitochondrial COI and ND2 genes.  
1000 *Mitochondrial DNA* 27, 3865–3875. <https://doi.org/10.3109/19401736.2014.971240>
- 1001 Watanabe, Y., Zenitani, H., Kimura, R., 1995. Population decline off the Japanese sardine *Sardinops*  
1002 *melanostictus* owing to recruitment failures. *Can. J. Fish. Aquat. Sci.* 52, 1609–1616.  
1003 <https://doi.org/10.1139/f95-154>
- 1004 Wickham, H., 2009. Introduction, in: *Ggplot2*. Springer New York, New York, NY, pp. 1–7.  
1005 [https://doi.org/10.1007/978-0-387-98141-3\\_1](https://doi.org/10.1007/978-0-387-98141-3_1)
- 1006 Xiaojin, X., Weijun, W., Weijian, Y., 2000. The life span of *Dactylogyrus vaginulatus* on

- 1007        *Hypophthalmichthys molitrix*. Journal Nanjing Agric. Univ. 22, 95–98.
- 1008    Yan, S., Wang, M., Yang, C.-P., Zhi, T.-T., Brown, C.L., Yang, T.-B., 2016. Comparative  
1009        phylogeography of two monogenean species (Mazocraeidae) on the host of chub mackerel,  
1010        *Scomber japonicus*, along the coast of China. Parasitology 143, 594–605.  
1011        <https://doi.org/10.1017/S0031182016000160>
- 1012    Zelditch, M., Swiderski, D.L., Sheets, H.D., 2012. Geometric morphometrics for biologists : a  
1013        primer. Elsevier, London.
- 1014
- 1015

1016 **Figure captions**



1017

1018 **Fig. 1: Sampling sites in Lake Tanganyika with an overview of significant results of morphometric**

1019 **(above arrow) and geomorphometrics (below arrow) analyses between the specimens of**

1020 ***Kapentagyrys* spp. from the respective sampling sites. A) *K. limnotrissae*, B) *K. tanganicus* ex *L.***

1021 ***miodon* and C) *K. tanganicus* ex *S. tanganicae*. The morphometric results are presented as the**

1022 **number of variables which differ between the respective sampling sites (before the dash) vs the**

1023 **total number of variables analysed (after the dash). In the case of geomorphometrics, the**

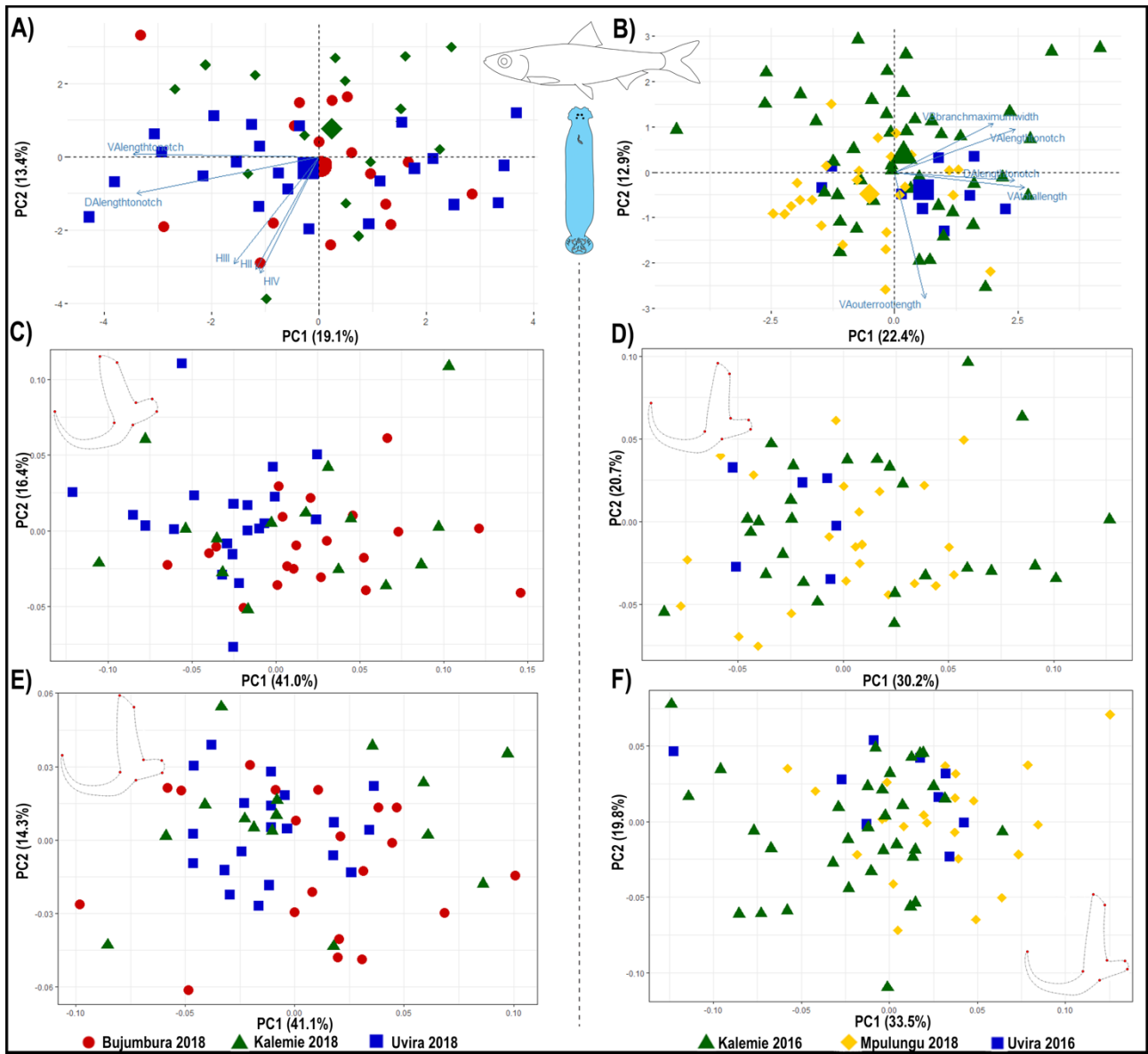
1024 **difference in either ventral, dorsal, both or none of the anchors is indicated. Shapes of signs**

1025 **correspond with the sampling site origin of specimens in the respective analyses. Colours of**

1026 **arrows refer to the separation on spatial (grey – ethanol preserved specimens) and spatio-**

1027 **temporal (black – fresh specimens) datasets. Map created using SimpleMappr software v7.0.0.**

1028 **(available at <http://www.simplemappr.net>. Accessed January 20, 2019).**



1029

1030

1031

1032

1033

1034

1035

1036

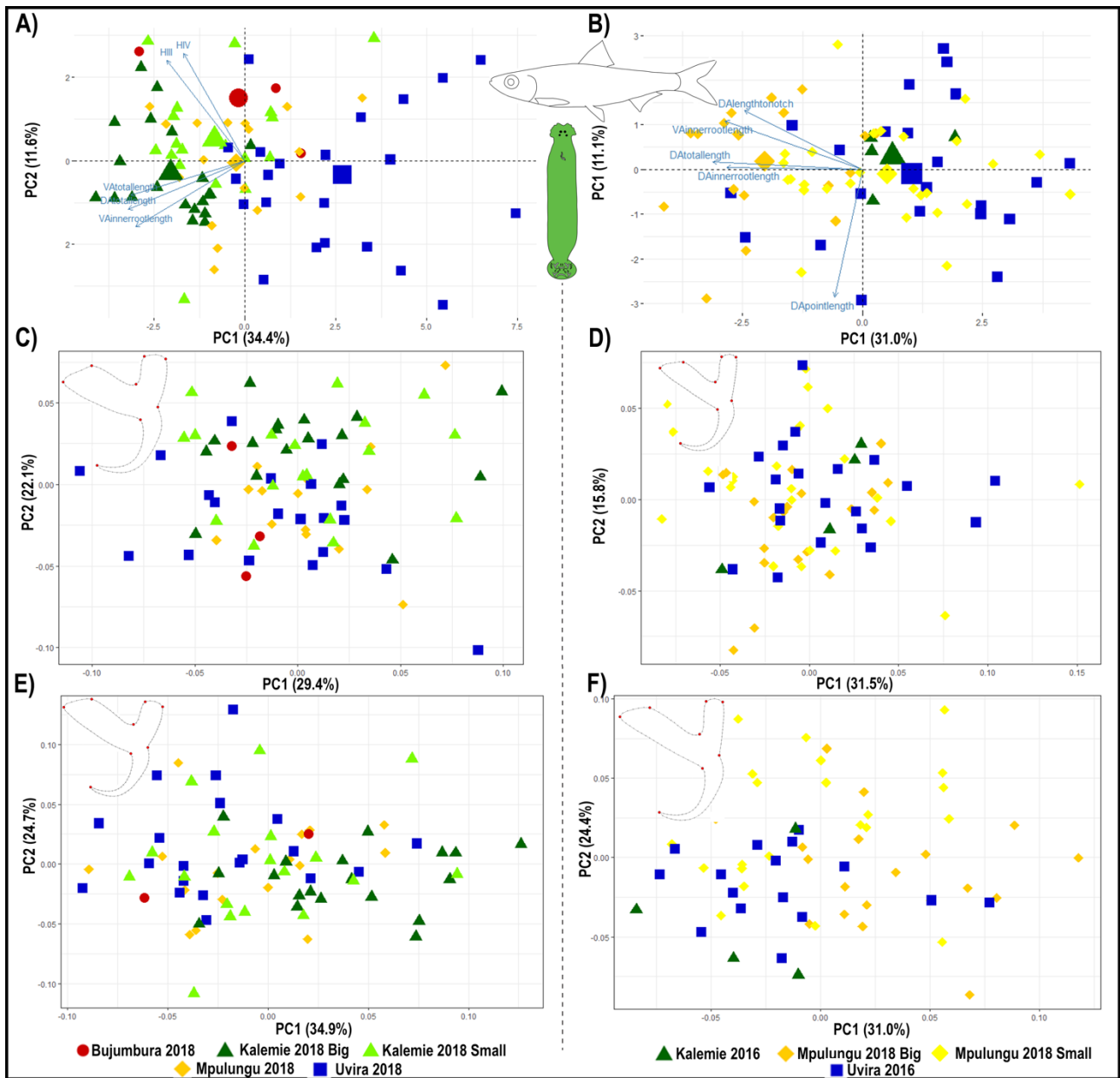
1037

1038

Fig. 2: Biplots showing the variation in haptoral structures of *K. limnotrissae*. Only the first two axes are shown. A) PCA of haptoral measurements with the five most contributing variables indicated by arrows, ethanol-preserved specimens (fifth and seventh pair of marginal hooks excluded due to missing data, the average position for each group is indicated by a larger size of the symbol); B) PCA of haptoral measurements with the five most contributing variables indicated by arrows, fresh specimens (second to seventh pair of marginal hooks excluded due to missing data, the average position for each group is indicated by a larger size of the symbol); C) PCA based on Procrustes distances of eight fixed landmarks describing the shape of the dorsal anchor, ethanol preserved specimens; D) PCA based on Procrustes distances of eight fixed landmarks

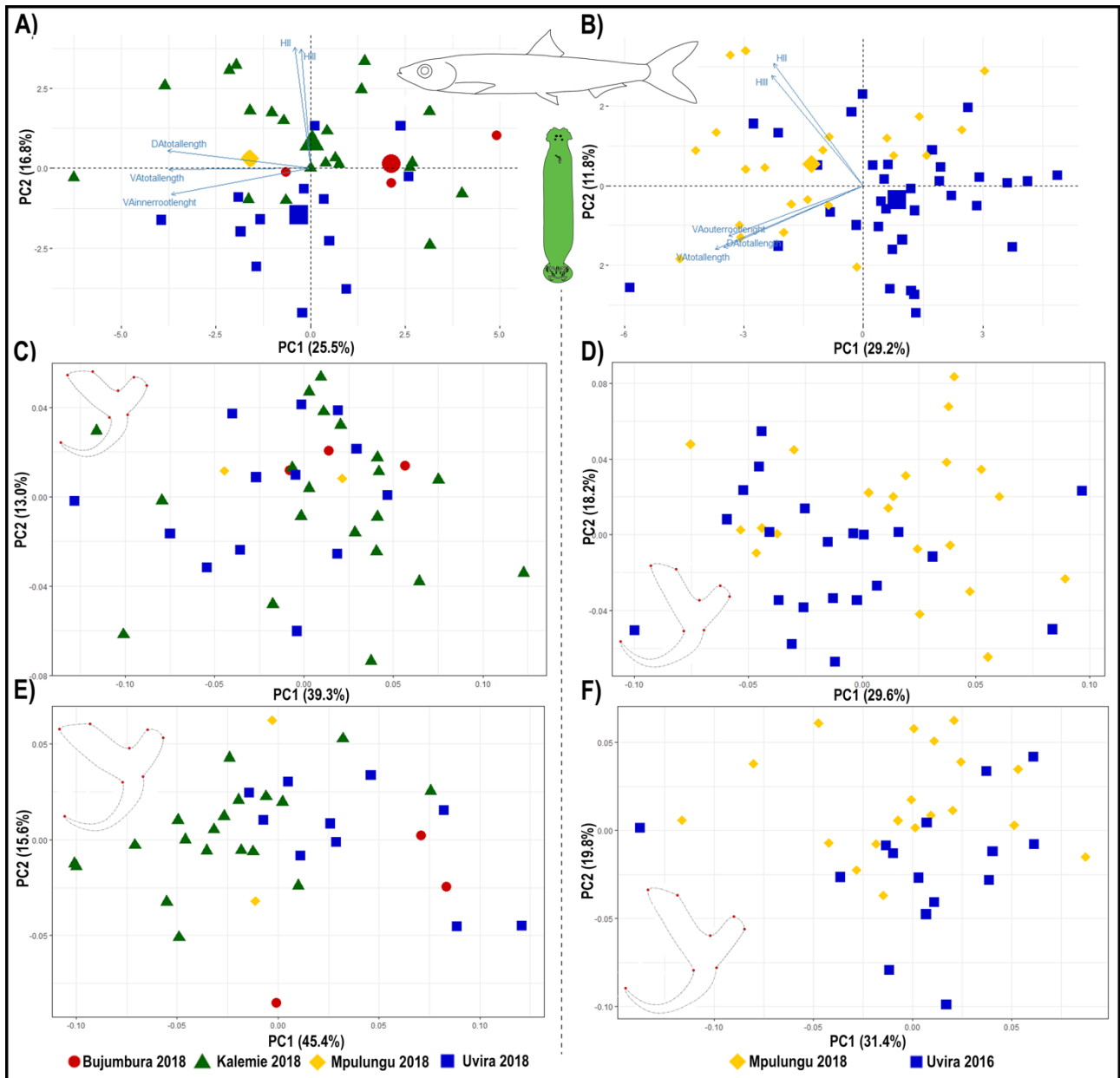


1039 describing the shape of the dorsal anchor, fresh specimens; E) PCA based on Procrustes distances  
 1040 of eight fixed landmarks describing the shape of the ventral anchor, ethanol preserved specimens;  
 1041 F) PCA based on Procrustes distances of eight fixed landmarks describing the shape of the ventral  
 1042 anchor, ethanol preserved specimens. Consensus anchor shape for the respective analysis is  
 1043 shown.



1044  
 1045 **Fig. 3: Biplots showing the variation in haptoral structures of *K. tanganicanus* collected from *L.***  
 1046 ***miodon* in this study. Only the first two axes are shown. A) PCA of haptoral measurements with**  
 1047 **the five most contributing variables indicated by arrows, ethanol-preserved specimens (fifth to**

1048 seventh pair of marginal hooks excluded due to missing data, the average position for each group,  
1049 is indicated by a larger size of the symbol); B) PCA of haptoral measurements with the five most  
1050 contributing variables indicated by arrows, fresh specimens (second to seventh pair of marginal  
1051 hooks excluded due to missing data, the average position for each group is indicated by a larger  
1052 size of the symbol); C) PCA based on Procrustes distances of eight fixed landmarks describing the  
1053 shape of the dorsal anchor, ethanol preserved specimens; D) PCA based on Procrustes distances of  
1054 eight fixed landmarks describing the shape of the dorsal anchor, fresh specimens; E) PCA based on  
1055 Procrustes distances of eight fixed landmarks describing the shape of the ventral anchor, ethanol  
1056 preserved specimens; F) PCA based on Procrustes distances of eight fixed landmarks describing  
1057 the shape of the ventral anchor, ethanol preserved specimens. Consensus anchor shape for the  
1058 respective analysis is shown.



1059

1060

1061

1062

1063

1064

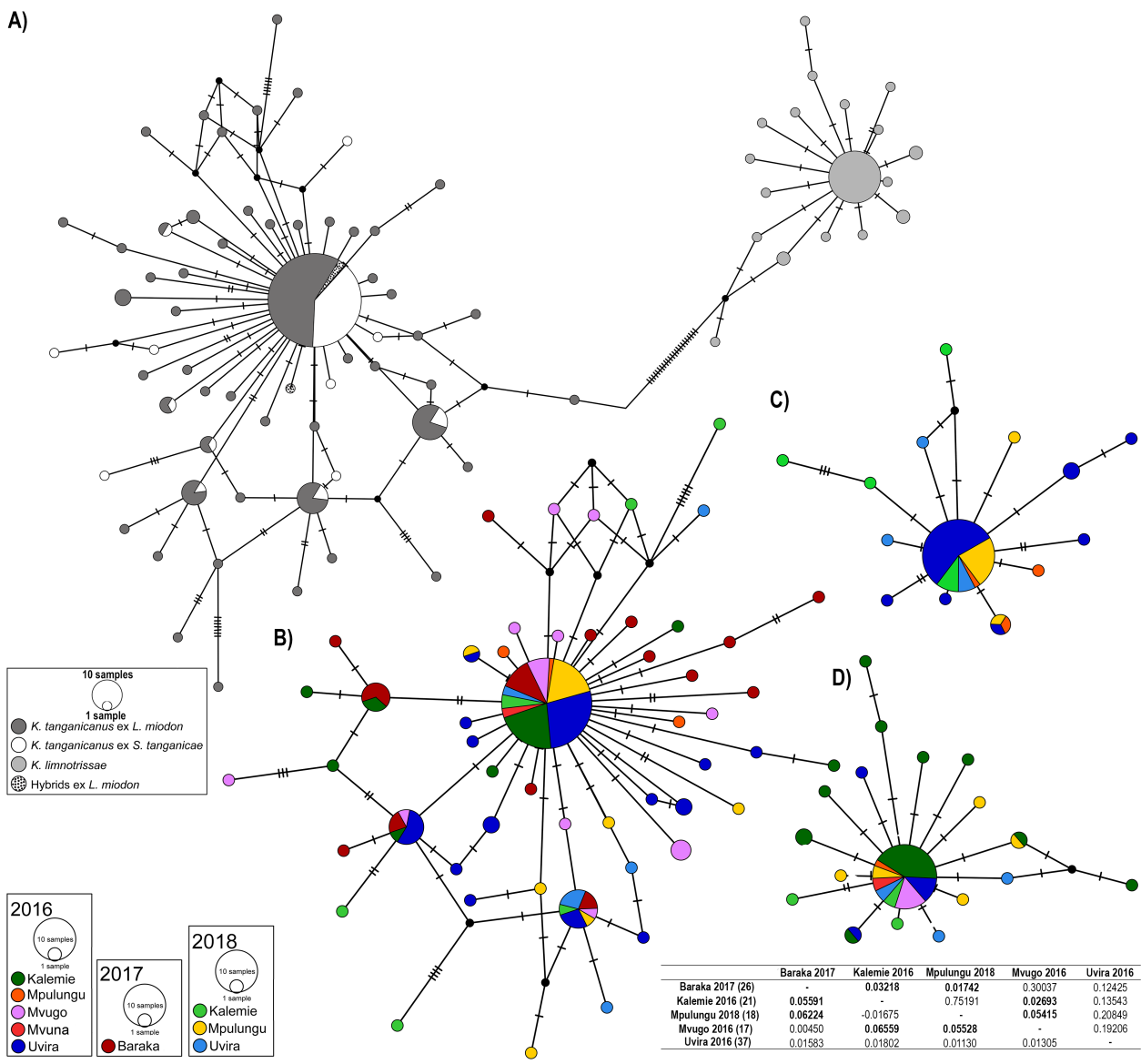
1065

1066

1067

**Fig. 4: Biplots showing the variation in haptoral structures of *K. tanganicus* collected from *S. tanganicae* in this study. Only the first two axes are shown. A) PCA of haptoral measurements with the five most contributing variables indicated by arrows, ethanol-preserved specimens (fifth and seventh pair of marginal hooks excluded due to missing data, the average position for each group is indicated by a larger size of the symbol); B) PCA of haptoral measurements with the five most contributing variables indicated by arrows, fresh specimens (sixth and seventh pair of marginal hooks excluded due to missing data, the average position for each group is indicated by a larger size of the symbol); C) PCA based on Procrustes distances of eight fixed landmarks**

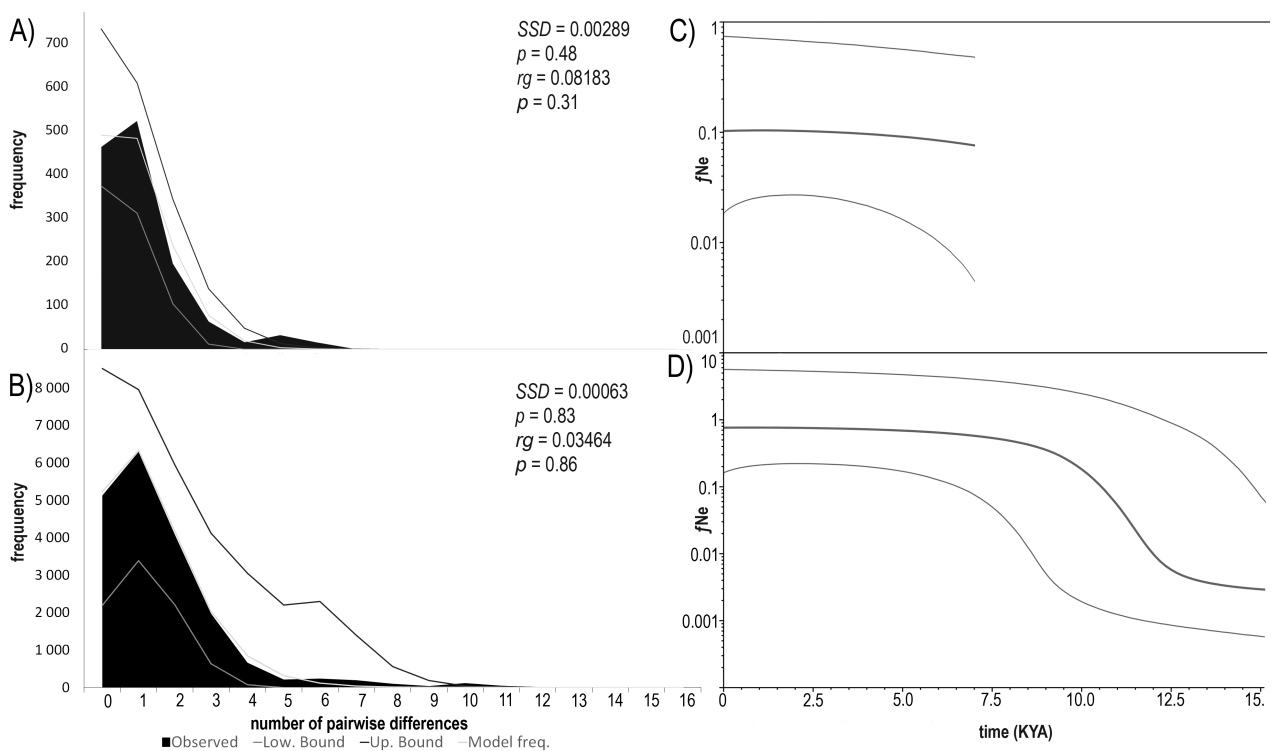
1068 describing the shape of the dorsal anchor, ethanol preserved specimens; D) PCA based on  
 1069 Procrustes distances of eight fixed landmarks describing the shape of the dorsal anchor, fresh  
 1070 specimens; E) PCA based on Procrustes distances of eight fixed landmarks describing the shape of  
 1071 the ventral anchor, ethanol preserved specimens; F) PCA based on Procrustes distances of eight  
 1072 fixed landmarks describing the shape of the ventral anchor, ethanol preserved specimens.  
 1073 Consensus anchor shape for the respective analysis is shown.



1074  
 1075 **Fig. 5: Genetic population structure of *Kapentagyris* spp. based on COI sequences (415 bp).**

1076 Median joining haplotype network of A) *K. tanganicanus* and *K. limnotrissae* with hybrid  
 1077 individuals; B) *K. tanganicanus* ex *L. miodon*; C) *K. tanganicanus* ex *S. tanganicae*; D) *K.*

1078 *limnotrissae*. The circles represent different haplotypes with their size proportional to the number  
 1079 of individuals represented. Haplotypes are connected with lines, indicating the number of  
 1080 mutations. Small black circles indicate hypothetical haplotypes, predicted by the model. Colours  
 1081 represent sampling events and host species, respectively, as mentioned in the legends. Genetic  
 1082 differentiation among geographically pre-defined subpopulations of *K. tanganicus* ex *L. miodon*  
 1083 listed in the enclosed table. Pairwise  $F_{ST}$  values and corresponding P-values are shown below and  
 1084 above the diagonal, respectively. Significant results with  $\alpha=0.05$  are marked in bold. Number of  
 1085 monogean individuals in brackets.



1086

1087 **Fig. 6: Demographic history of *Kapentagyrus* spp.** Mismatch distribution for A) *K. limnotrissae* and  
 1088 B) *K. tanganicus*. The black bars show the observed frequency of pairwise differences. The grey  
 1089 lines refer to the expected distribution based on parameter estimates (plus 95% confidence limits)  
 1090 under a model of population growth. The sum of squared differences (SSD) and the raggedness  
 1091 index (rg) and their respective p-values are given to describe the fit of the observed distribution to  
 1092 the expectations based on growth parameter estimates, as well as  $\tau$ , the modal value of the

1093 mismatch distribution. Bayesian Skyline plot (BSP) of C) *K. limnotrissae* based on 415 base pairs of  
1094 COI sequences and D) *K. tanganicus* based on 415 base pairs of COI sequences. BSPs show the  
1095 effective populations size through time, assuming a substitution rate of 10% per site per million  
1096 years in *Kapentagyris* spp. The thick line represents the median values; the thin lines denote 95%  
1097 highest posterior density (HPD) intervals. The y-axis represents the population size parameter  
1098 (product of female effective population size,  $fN_e$ , and mutation rate,  $\mu$ ).

1099 Table 1: Number of fish specimens of (a) *Limnothrissa miodon* and (b) *Stolothrissa tanganicae* examined for monogenean parasites along with sampling  
 1100 site, basin and infection parameters. Values for *Kapentagyris limnothrissae* and *Kapentagyris tanganicanus* are shown before and after the dash,  
 1101 respectively).

Sampling site (geographic coordinates, date, year)	Locality – basins (Danley et al. 2012)	Number of fish specimens	Number of monogenean individuals	Prevalence (%)	Infection intensity	Abundance (range)	Number of COI haplotypes (Genbank a.n)	Number of microscopic slides (a.n. in HU)
<b>(a) <i>Limnothrissa miodon</i></b>								
Baraka (4°05'S–29°06'E; 29.7.2017)	The northern basin	24	10/63	16.7/41.7	2.5/5.4	0.4 (0–4)/2.1 (0–15)	–/26 (MK598222–47)	–/–
Bujumbura (3°23'S– 29°22'E; 10.4.2018)	The northern basin	30	108/4	83/10	4.3/1.3	3.6 (0–17)/ 0.1 (0–2)	–/–	X.4.13–37/ XII.2.10–13
Kalemie (5°56'S–29°12'E; 12.8.2016)	The central basin	10	55/5	80/33	6.9/1.7	5.5 (0–15)/0.5(0–2)	23 (MK598078–100)/21 (MK598145–65)	XI.1.11–2.12/ XI.3.49–50, 4.01–2, 19–20
Kalemie (12.4.2018)	The central basin	20	24/204	25/70	4.8/14.6	1.2 (0–11)/ 10.2 (0–37)	4 (MK598125–28)/8 (MK598137–44)	X.3.45–4.12/ XI.4.21, XII.1.01–38
Mpulungu (8°46'S– 31°07'E; 19.8.2016)	The southern basin	2	1/3	50/50	1/3	0.5(0–1)/1.5(0–3)	1 (MK598114)/3 (MK598248–50)	XI.2.21–22/–
Mpulungu (7.4. – 21.4.2018)	The southern basin	81	60/452	28/63	2.6/9	0.7 (0–8)/ 5.6 (0–42)	6 (MK598115–20)/18 (MK598251–68)	X.3.26–44/ XI.4.22–50, XII.2.10–28
Mvugo (4°18'S–29°34'E. 4.8.2016)	The northern basin	6	9/25	50/100	3/4.2	1.5 (0–3)/4.2 (1–10)	2 (MK598112–13)/17 (MK598205-21)	XI.2.13–20/ XI.4.03–18
Mvuna Island (7°26'S– 30°36'E 1.4.2015)	The southern basin	6	11/5	50/50	3.7/1.7	1.8 (0–8)/0.8 (0–3)	5 (MK598101–5) /2 (MK59817–8)	XI.2.33–37/–
Uvira (3°22' S–29°08'E; 11.8.2016)	The northern basin	41	12/28	35/40	1.7/3.5	0.6 (0–3)/1.4(0–9)	6 (MK598106–11)/37 (MK598166–76, 79–204)	XI.1.11–20/ XI.3.26–48
Uvira (12.4.2018)	The northern basin	30	43/70	53/76.7	2.7/3.0	1.4 (0–7)/ 2.3 (0–8)	4 (MK598121-24)/8 (MK598129-36)	X.4.38–50, XI.1.01–10/ XII.1.39–2.09
<b>(b) <i>Stolothrissa tanganicae</i></b>								
Bujumbura (10.4.2018)	The northern basin	30	5	16.7	1	0.17 (0–1)	–	XII.3.48–3.50
Kalemie (11.8.2016)	The central basin	33	0	0	0	0	–	-
Kalemie (12.4.2018)	The central basin	30	44	66.7	2.2	1.5 (0–5)	7 (MK598317–23)	XII.3.26–3.47
Mpulungu (19.8.2016)	The southern basin	18	3	16.7	1	0.17 (0–1)	3 (MK598269, 81–82)	XII.4.24–25
Mpulungu (7.4. – 21.4.2018)	The southern basin	84	107	52.4	2.4	1.3 (0–13)	11 (MK598270–80)	XII.3.15–3.25, 4.01–2

<b>Uvira (11.8.2016)</b>	The northern basin	27	31	44	2.6	1.1 (0–6)	29 (MK598283–311)	XII.2.38–3.10
<b>Uvira (12.4.2018)</b>	The northern basin	25	12	28	1.7	0.5 (0–3)	5 (MK598312–16)	XII.4.03–15

1102

1103 Table 2: Genetic diversity indices of species of *Kapentagyris*, and their hosts *Limnothrissa miodon* and *Stolothrissa tanganicae* (De Keyzer et al.,  
1104 2019) inferred from the COI mtDNA region.

Species	N	H	S	Hd	$\pi$	Max. divergence (%)
<i>K. limnothrissae</i>	51	19	18	0.6329±0.0800	0.002241±0.001742	1.2
<i>K. tanganicanus</i>	195	60	68	0.7341±0.0348	0.003800±0.002515	3.1
<i>K. tanganicanus</i> ex <i>L. miodon</i>	140	53	64	0.8066±0.0339	0.004499±0.002869	3.1
<i>K. tanganicanus</i> ex <i>S. tanganicae</i>	55	14	17	0.4983±0.0838	0.001991±0.001604	1.4
<i>L. miodon</i>	69	38	45	0.9250±0.0236	0.008909±0.004799	3.2
<i>S. tanganicae</i>	96	46	48	0.8583±0.0337	0.003543±0.002174	1.2

1105 N sample size, H number of haplotypes, S number of polymorphic sites, Hd haplotype diversity,  $\pi$  nucleotide diversity.

1106